OTH 90 317

HSE
Health & Safety Executive

THE EFFECT OF SHIP IMPACT ON THE LOAD CARRYING CAPACITY OF STEEL TUBES

Prepared by University of Strathclyde
for the Health and Safety Executive

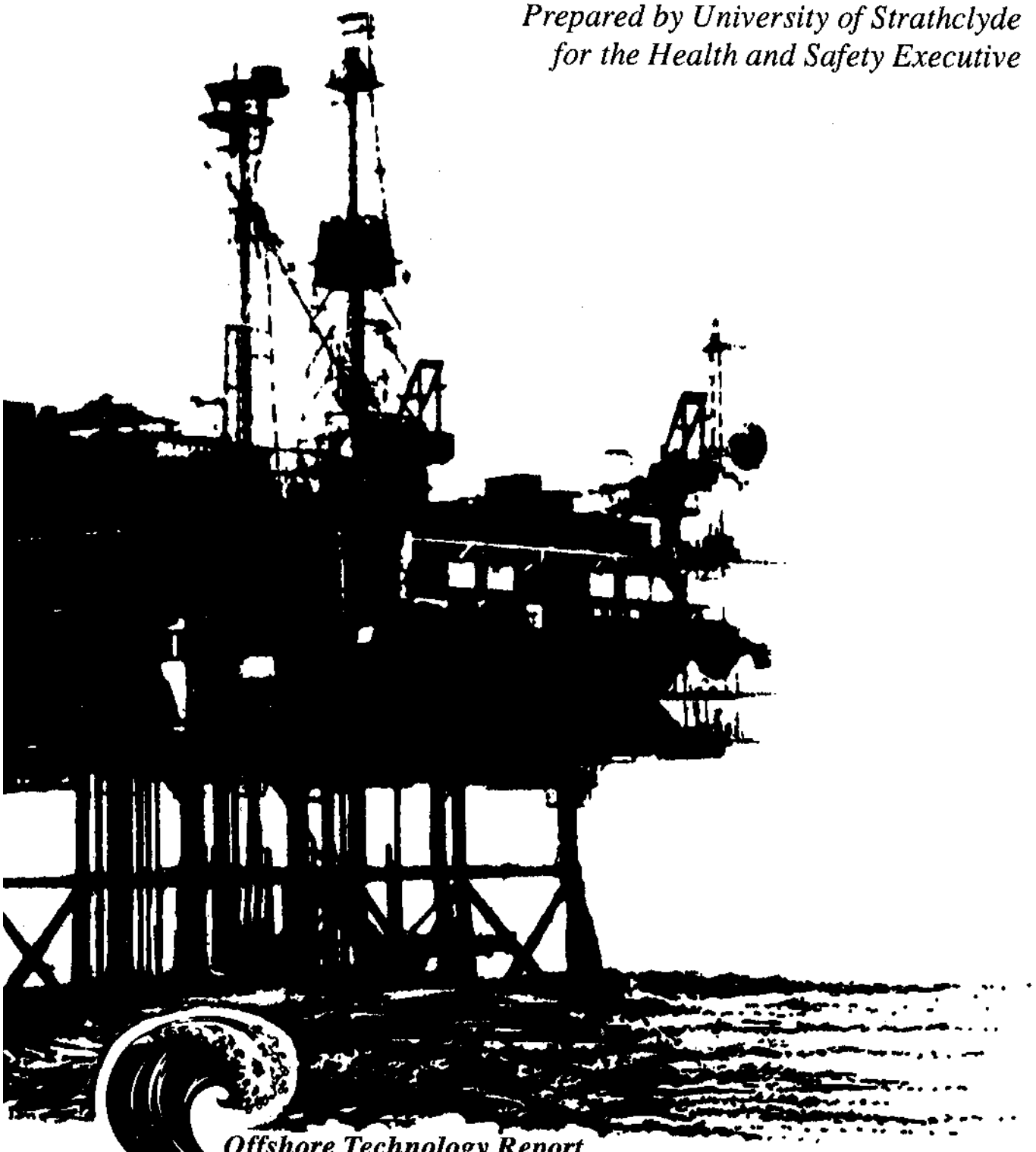

Offshore Technology Report

Health and Safety Executive

OTH 90 317

THE EFFECT OF SHIP IMPACT ON THE LOAD CARRYING CAPACITY OF STEEL TUBES

Authors

J D Allan and J Marshall

Department of Civil Engineering
University of Strathclyde
John Anderson Building
107 Rottenrow
East Glasgow

London: HMSO

Health and Safety Executive - Offshore Technology Report

First published 1992
ISBN 0 11 882130 X

This report is published by the Health and Safety Executive as part of a series of reports of work which has been supported by funds formerly provided by the Department of Energy and lately by the Executive. Neither the Executive, the Department nor the contractors concerned assume any liability for the reports nor do they necessarily reflect the views or policy of the Executive or the Department.

Results, including detailed evaluation and, where relevant, recommendations stemming from their research projects are published in the OTH series of reports.

Background information and data arising from these research projects are published in the OTI series of reports.

CONTENTS

SUMMARY

This is an extension of the study on the effect of ship collision on large diameter tubulars which was reported in the Department of Energy Report No OTI 88 532. Further tests and measurements have been carried out on the tubes used in that study to determine the effect of the damage on their capacity for carrying axial load.

The tubes were profiled around the region of damage and the depth, length and volume of the associated dent were measured. The depths of the dents were compared with those presented in the previous report; good correlation was obtained. The lengths of the dents were compared with lengths calculated from empirical expressions derived by others; little correlation was obtained. The volumes of the dents were compared with volumes calculated from empirical expressions derived by others; no correlation was obtained.

The support frame used for the impact tests in the previous work was modified to allow the application of concentric axial loading. This allowed the same restraint conditions to be applied to each tube as was used in the impact tests. The load was applied at a constant strain rate to failure.

An approximate analysis for the failure of a tube with dent and residual deflection was developed. The results predicted by this method were compared with those obtained experimentally; a good correlation was obtained.

The results of typical tests are shown graphically and the results of all tests are presented in tabular form.

1. INTRODUCTION

The mechanisms by which the steel tubulars which form the legs and bracing members of steel offshore jackets absorb the impact energy of ship collision were studied by Allan and Marshall [1] in a project funded by the Department of Energy. At the conclusion of that work a large number of damaged tubes remained each of which had absorbed an impact of known energy by mechanisms which had been recorded in detail.

The object of the work reported here was to quantify the dent damage sustained by each of these tubes, to apply an axially compressive load to failure of the tube and to examine the effect of the impact damage on the load carrying capacity of the tube. This work involved both laboratory testing and theoretical analysis.

A profiling rig was constructed to measure, and permanently record, the shape of the dents. In particular, the depth of the dent, the length of the dent and the shape of the dent were measured. From this information the change in volume of the tube due to the impact was calculated.

The tube support frame which restrained the tubes during the axial load tests was that used for the impact tests. A detailed description of this frame, and of the electronic monitoring equipment, is given in report OTI 88 532.

A loading rig was constructed to transfer the compressive load from a Dartec testing machine to the test specimen in the support frame. This rig allowed load to be applied at at a constant rate of strain. The central lateral deflection and the axial change in length were measured. Strain was recorded at the same four locations as for the impact tests.

The dent depth obtained from profiling is compared with that calculated from the impact tests and dent length is compared with a hypothetical definition. A simplified method for calculating the ultimate axial load carrying capacity of damaged tubulars is proposed. In addition to allowing for different end conditions, the analysis takes account of the contributions from dent depth and residual deflection on the reduction in load carrying capacity. The results obtained from this analysis are compared with the data obtained from the test programme.

It is not the intention of this report to present a detailed analysis of all the data amassed on the effect of impact on load carrying capacity. Rather it presents a general view of the effect of denting and residual deflection on axial load carrying capacity. The report should be read in conjunction with OTI 88 532 where full details of the test specimens and the results of the impact tests are given.

2. PROFILING

2.1 PROFILING RIG

2.1.1 General

The profiling process consisted of determining the cross sectional shape of the tube at a series of cross sections. The rig which was designed to carry out this operation can be considered under the headings:

- support frame which held the tube during profiling
- carriages on which the instrumentation for profiling was mounted
- instrumentation which measured and recorded displacements

2.1.2 Support frame

The steel frame shown in Figure 1 was constructed from Rectangular Hollow Section. The frame consisted of two U-form support cradles connected together by two parallel longitudinal sections. These sections were securely fixed to a rigid steel table. Figure 1 also shows the position of the aluminium carriage rails relative to the support frame.

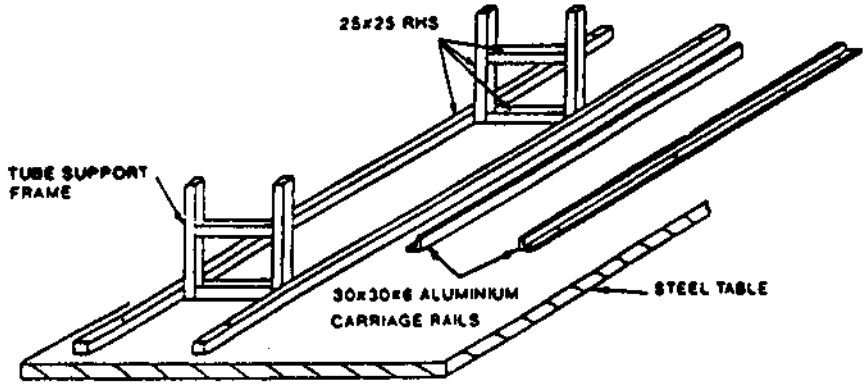

Figure 1
Support frame

2.1.3 Carriages

Two carriages were used to support the measuring equipment: the longitudinal carriage which moved on rails along the length of the tube, and the transverse carriage, mounted on a parallel slide unit on the longitudinal carriage, which moved across the tube.

Two calipers were fitted to a vertical post which was fixed to the moving part of the slide unit. The calipers consisted of two sliding cantilever brackets. The tracking points of the brackets were angled and capped with small round steel balls. The brackets were connected together by a clamp spring which was designed to hold the points tightly against the surface of the tube being profiled. A balance spring connected the top bracket to the vertical post and an electric motor, mounted on the longitudinal carriage, drove the transverse carriage at a controlled and constant speed across the tube. The arrangement of the carriages is shown in Figure 2.

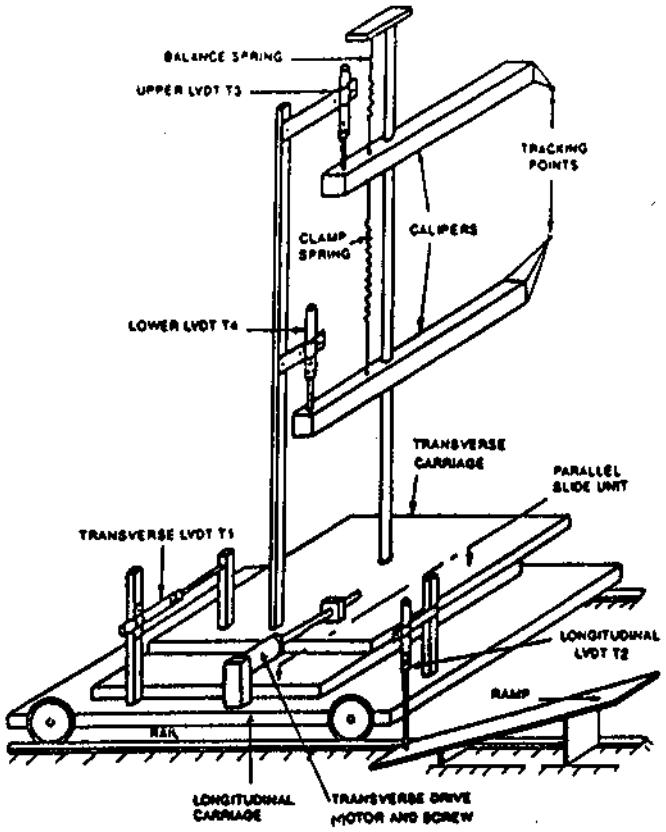

Figure 2
Schematic arrangement of carriages

2.1.4 Instrumentation

All movements were measured using Linear Variable Displacement Transducers(LVDT). Four transducers were involved. Their positions are shown in Figure 2 where they are given the location numbers T1, T2, T3 and T4.

Transducer T1, mounted horizontally on the longitudinal carriage, measured the movement of the transverse carriage. Transducer T2, mounted on the longitudinal carriage, measured longitudinal movement indirectly by measuring rise up an inclined ramp which was attached to the steel table. Transducers T3 and T4 profiled one symmetrical quarter of the dent by measuring the vertical displacement of each of the caliper brackets relative to the transverse slide.

The signals from the LVDTs were transmitted through an analogue to digital converter to a micro-computer for interpretation and storage. The computer was also programmed to control the profiling operation.

2.2 PROCEDURE

2.2.1 General

The length of tube profiled depended on the extent of the dent. However in all cases the tube was profiled at least 100 mm beyond what was judged to be the dent length.

During a traverse across a section, the computer was programmed to take readings automatically. Transverse increments were controlled by the readings from transducer T1 which was monitored continuously. As control was based on the horizontal movement two increments of movement were necessary. The traverse was always carried out from the centre line of the tube. Initially readings were taken at 2 mm intervals but this was changed to 0.5 mm as the calipers travelled down the face of the tube. The end of the traverse was defined when the points of the calipers came together.

2.2.2 Method

The method of profiling a symmetrical quarter of a tube, and the computer operations involved were:

- The tube was placed in the U-form cradles with the dent horizontal and facing upwards and the transverse and longitudinal centre lines of the dent marked. The tube was positioned with the dent located centrally between the cradles.
- The points of the calipers were brought together at a convenient longitudinal and transverse location and readings were taken on transducers T3 and T4 to establish an origin from which relative deflections could be calculated.
- The calipers were located with the top transducer (T3) on the centre of the dent and readings were taken on all transducers. This established the origins for all transducers relative to the tube.
- The calipers were manually moved back from the transverse origin, the traverse motor started and continuous computer monitoring of the traverse begun. Readings were taken from the caliper transducers (T3 and T4) at predetermined increments from the point at which the transverse origin was passed.
- The profiling rig was moved longitudinally to the next section and the calipers located behind the transverse origin. A reading was taken to establish the longitudinal coordinate of the section and automatic transverse recording was initiated.

2.3 RESULTS

2.3.1 General

The greatest achievable accuracy in profiling was dependent on the accuracy of the analogue to digital conversion. This was of the order of 0.05 mm.

On a very limited number of occaisions the deformed shape of the tube gave rise to difficulties in alignment on the support rig. In these cases it was found that the transverse centre of the dent was out of line with the centre of the cradles. This implied that the tube was bent normal to the axis of the dent.

The largest error arose from the geometric variation in the point of contact between the rounded points of the calipers and the surface of the tube as the calipers travelled round the tube. The largest error from any source was of the order of 0.2 mm; this occurring at the outer edge of the traverse.

The results for dent depth, length and volume change for every specimen profiled are given in Appendix A.

2.3.2 Typical profiles

Typical profiles for specimens with large and small dents from the round indenter are given Figure 3 and Figure 4 respectively. These plots show the cross section of a symetrical half of a tube.

The sections, while not equally spaced along the tube, give a good impression of the form of the dent. The nominal tube diameter was calculated from the profiling results on the assumption that the last section profiled was clear of the dent deformation.

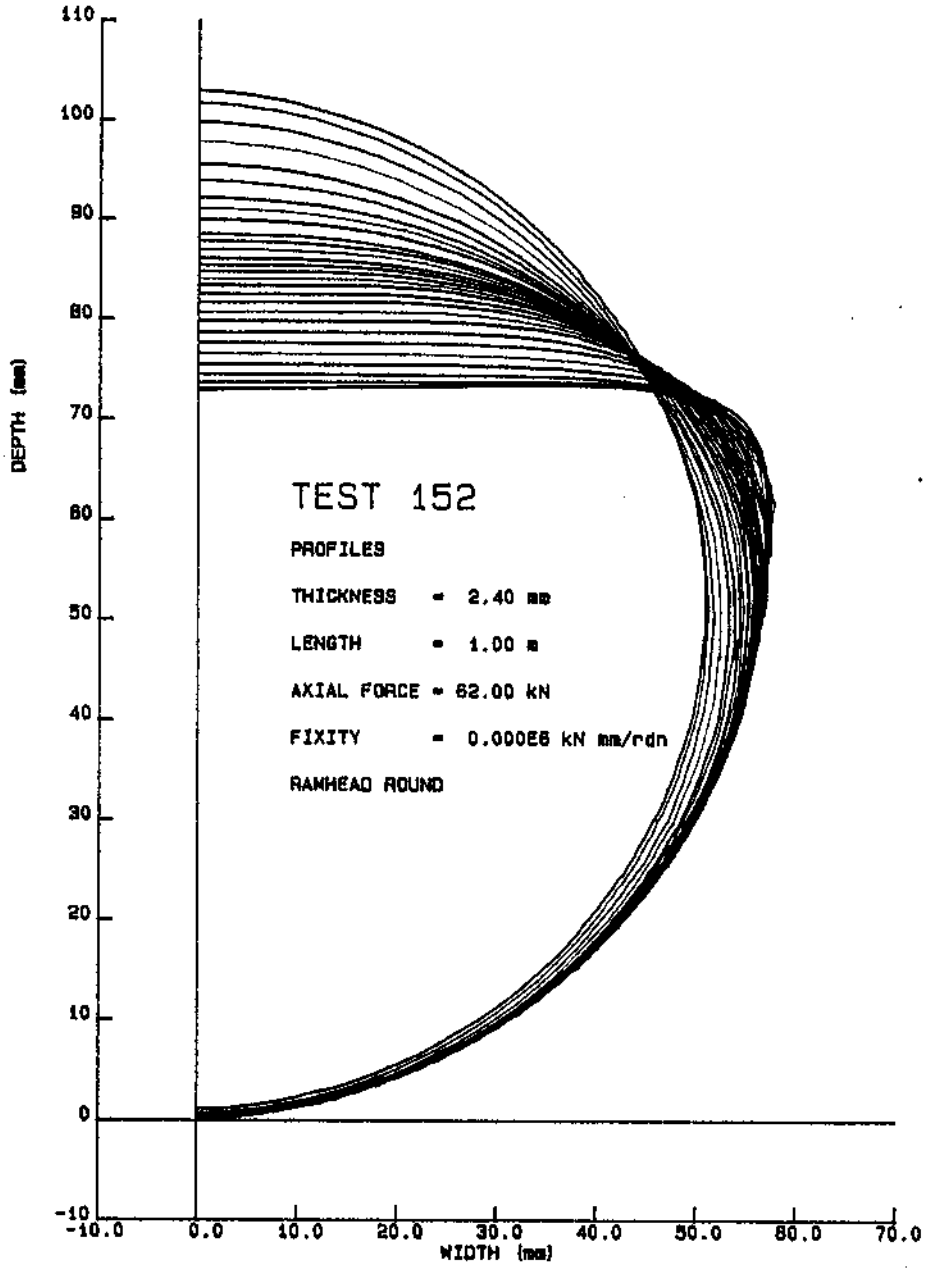

Figure 3
Typical profile of a thin walled tube

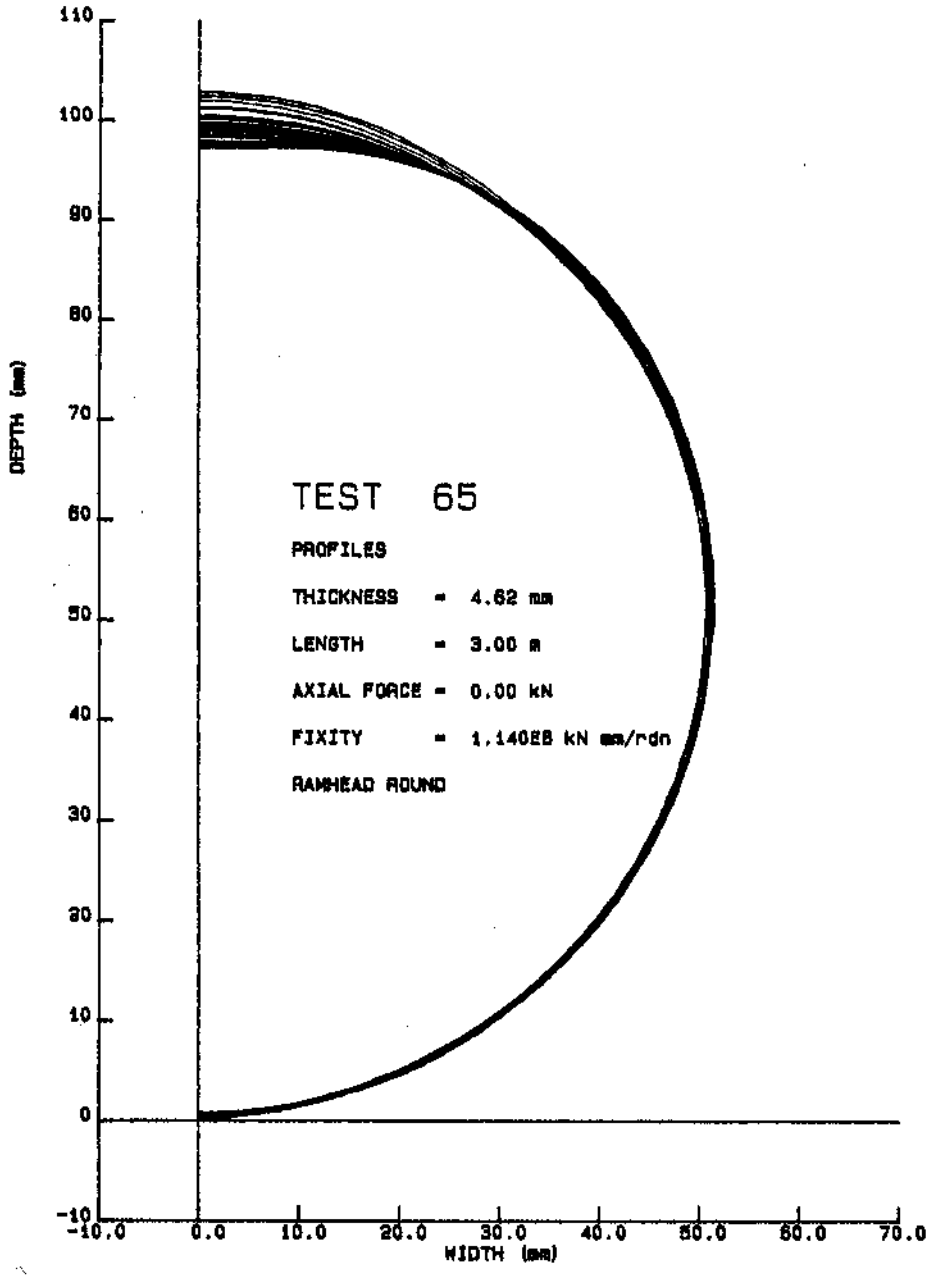

Figure 4
Typical profile of a thick walled tube

2.3.3 Dent depth

The nominal tube diameter was taken to be the distance between transducers T3 and T4 with the transducers on the centre line of the tube at the last section traversed.

Calculation of the depth of dent created by the round indenter was based on the average of readings taken close to the centre of the dent. The distance between the transducers T3 and T4 was calculated at the centre of the dent and at 2 mm away from the centre. The average of these distances was taken to be the minimum diametric distance. The maximum dent depth was obtained by subtracting this distance from the nominal tube diameter.

The definition of the depth of dent caused by the flat indenter was more difficult to define. it was found that, generally, the maximum dent did not occur at the centre of the span but was found to be at the edge of the indenter. This was some 150 mm from the centreline. In such cases the definition of dent depth was taken to be the maximum found from all cross section profiles.

A survey of the profiling results in Appenedix A shows that, for tubes of the same span and thickness, there was very little variation in the measured dent depths . Generally the deviations about the mean for any group were of the same order. This would indicate that neither the ranges of axial pre-load nor the end rotational restraints used in the dynamic tests have a significant influence on the dent characteristics.

A comparison of the dent depths calculated from the profiling and from the dynamic tests is given in Figure 5.

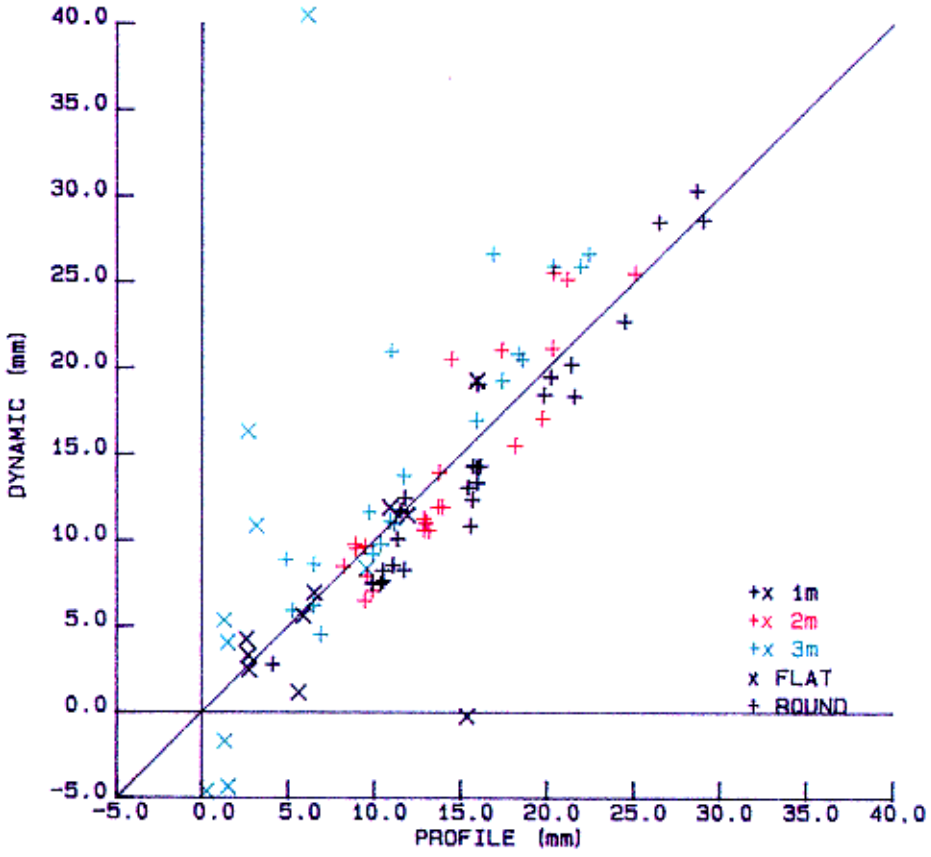

Figure 5
Comparison of dent depths

Generally there is reasonable agreement for those results from the round indenter. However there are many sources of error in the calculation of dent depth from the dynamic tests; these include the definition of zero force, the integration of the digitised signal from the tachogenerator and the analysis of the signal from the transverse transducer.

The results from the tests with the flat impactor show a wide scatter. There is an incompatibility between the criteria used to define maximum dent from profiling and that used for the dynamic tests. A typical longitudinal section from a plate impactor test is shown in Figure 6.

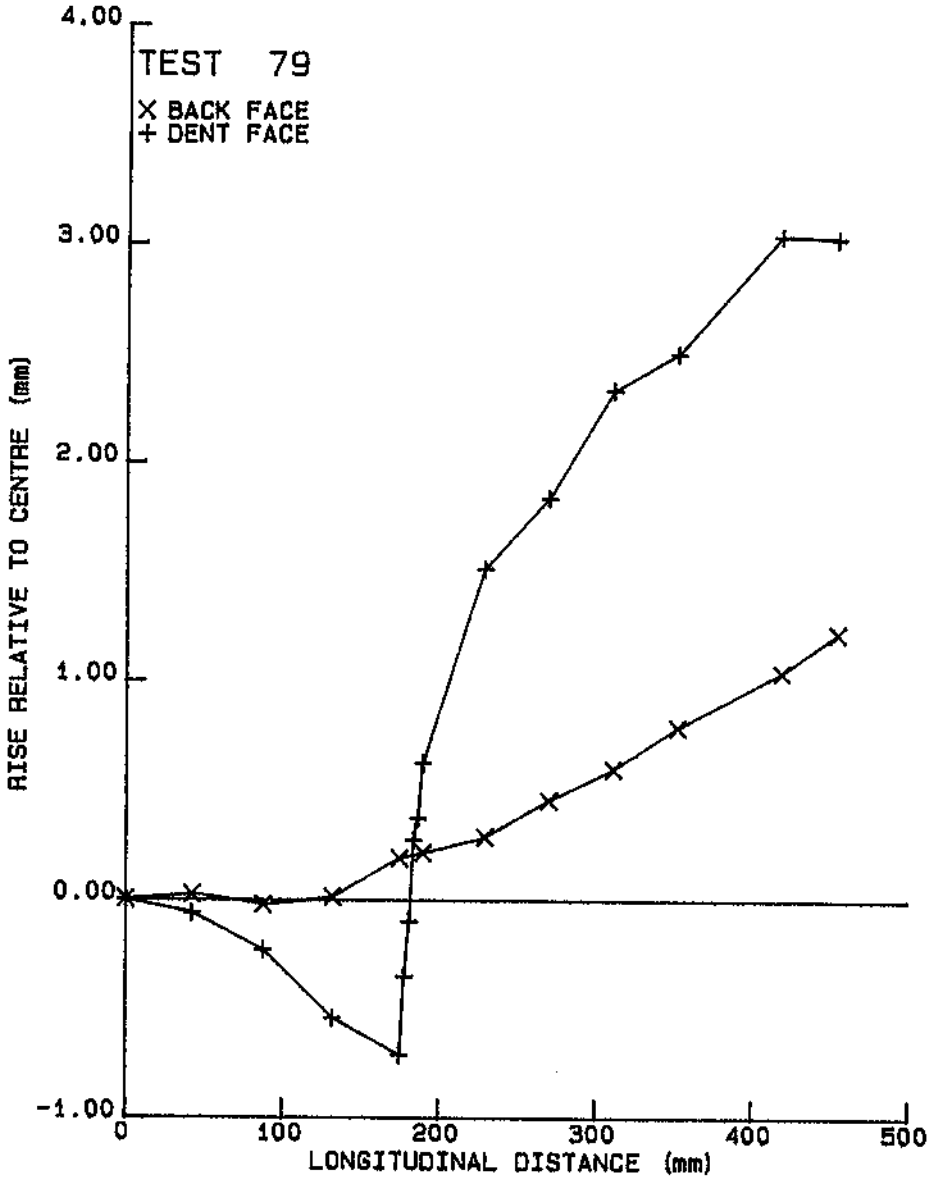

Figure 6
Plate impactor
Typical longitudinal profile

The dent face profile indicates a complex cross section deformation variation within the length of the plate impactor. Measuring the dent at the centreline of the tube results in a negative dent. Negative results were also obtained from the dynamic tests which were larger than those obtained from profiling. These results indicate an initial ovalisation of the tube which is less at the dent than at the last section profiled.

2.3.4 Dent length

An expression defining the profile of a dent is given in Reference 2 as:

$$d = DDe^{-1.3x/D} \qquad \text{Eqn 1}$$

where d = dent depth at a distance x from the dent centre line
DD = maximum dent at the centre line
D = nominal tube diameter.

The length of the dent was considered to be that at which the dent depth reduced to 1% of the maximum depth. The length of dent is then given by:

$$DL = 3.5D \qquad \text{Eqn 2}$$

where DL = dent length

While the profiling readings are confused by the initial ovality of the tube and by the ovality consequent on the impact, the accuracy of the profiling is estimated to be within 1% of the dent depth. Therefore when the results obtained from profiling were compared with the results obtained from Equation 1 the dent length was defined from the section at which the dent depth had reduced to 5% of the maximum.

The dent lengths, shown in Appendix A, are consistent within the groupings of wall thickness and span.

In Figure 7, the dimensionless parameter span over diameter (L/D) is plotted against the dimensionless parameter dent depth over diameter (DD/D). As calculated from Equation 1, the section at which the depth of the dent reduces to 5% of maximum occurs at a distance of 1.15D from the centreline. The value of 2.3D is used for the dent length and this is plotted on Figure 7. With few exceptions, the results from the round ram show a definite trend of disproportionate increasing length with dent depth.

The results obtained from the flat ram were inconclusive. The dent profiles bore little relationship to those obtained from Equation 1 and no correlation between individual profiling results was apparent.

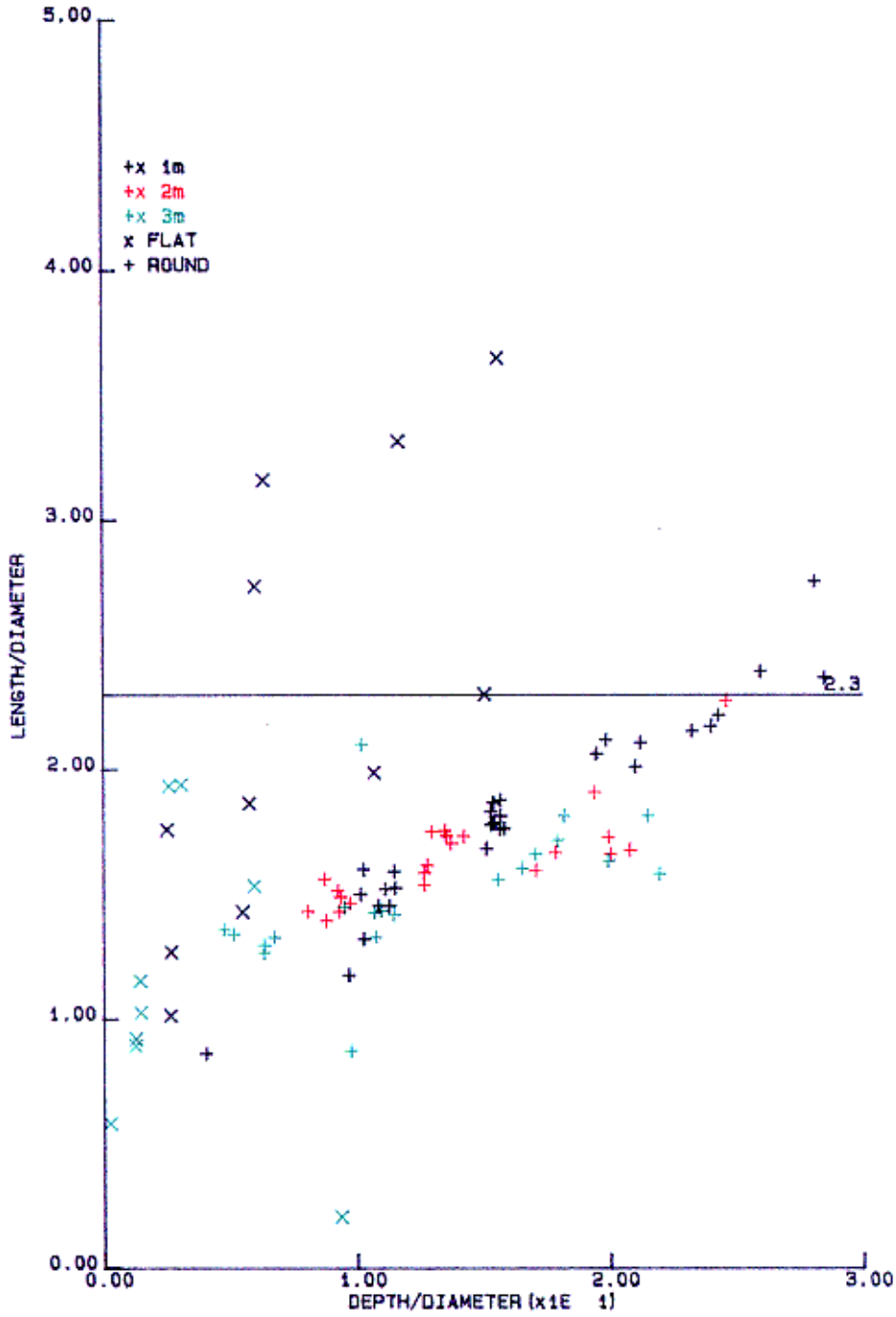

Figure 7
Variation in dent depth with length

2.4.5 Dent volume change

In Figure 8 the dimensionless parameter Reduced volume over Original volume (Vr/Vo) is plotted against the dimensionless parameter Dent depth over Diameter(DD/D). The reduced volume was calculated by integrating the separation between transducers T3 and T4 over both longitudinal and transverse increments. An allowance for the volume of the arc was added to the last readings at each section. The original nominal volume was calculated from the product of nominal mean diameter times the distance to the last section profiled. No account of residual bending in the tube was taken when calculating this volume.

Errors in calculating the nominal volume might result when large residual deflections accompany small dent sizes and from axial shortening of the tube due to large dents. It is felt that profiling is not the best way to measure volume change.

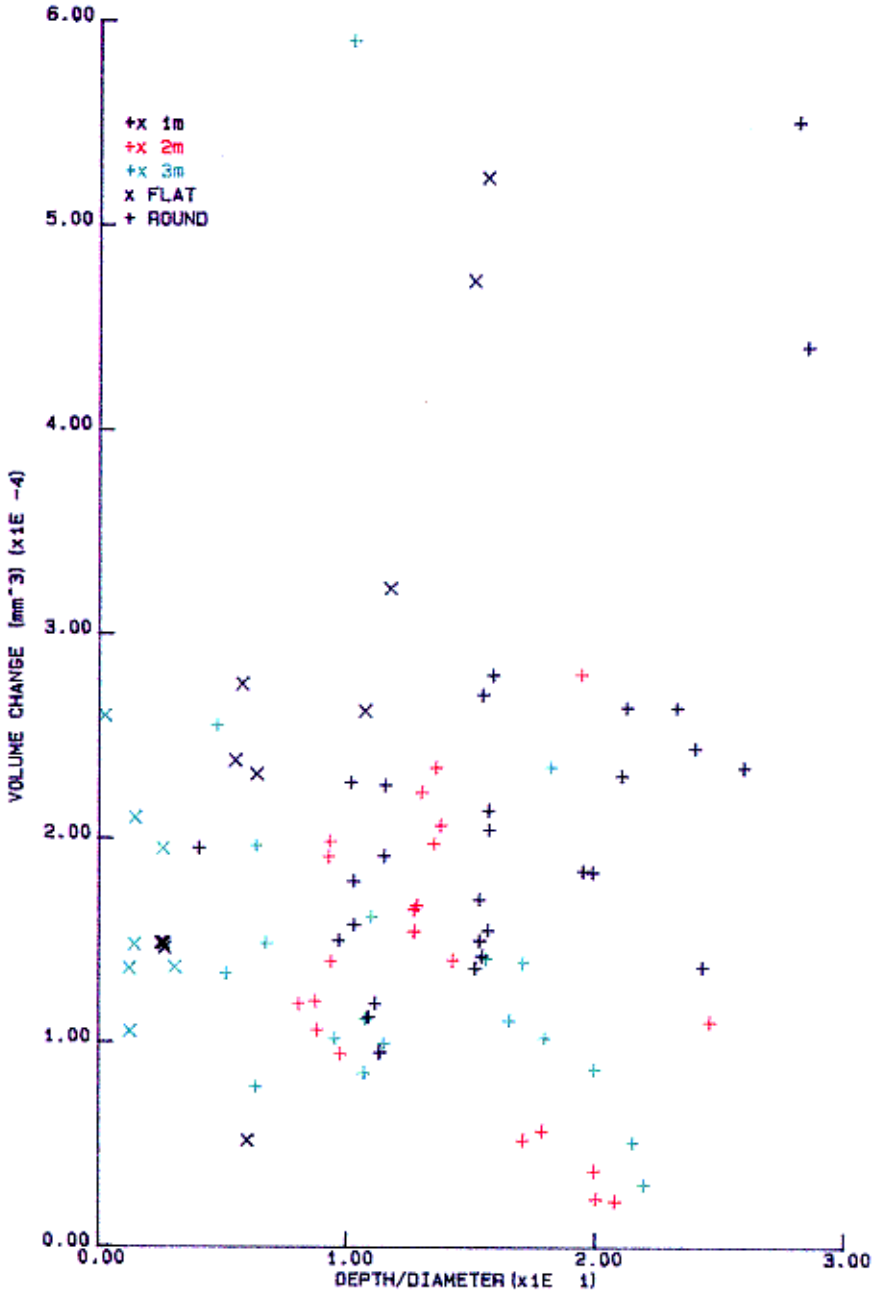

Figure 8
Volume change with dent depth

3. AXIAL TESTS

3.1 LABORATORY EQUIPMENT

3.1.1 General

The loading specification for the tests was that the apparatus deliver compressive loads up to a maximum of 1000 kN over a stroke distance of 50 mm under stroke control and at rates of stroke which would result in strain rates below 20 μstrainper second in the test specimens. Each tube was to be tested under the same conditions of end restraint as pertained for the dynamic test. Load, axial displacment, axial strain and lateral displacement at the centre line were to be monitored throughout the test.

The equipment used is described under the headings:

- Support frame
- Loading rig
- Instrumentation

3.1.2 Support frame

The frame used for the dynamic tests was again used here. the design of the frame was governed by the requirements of the end support conditions; fully fixed in the transverse or shear direction, free in the longitudinal or axial direction, both fully fixed rotationally and with rotational restraint related to the bending stiffness of the test piece. The frame is shown in Figure 9.

T-pieces were adopted to achieve the required end conditions. Rotational constraint was provided by the flexural action of members framing into the T-pieces. These restraining tubes were held at their remote ends by a tie beam. The degree of rotational restraint was provided by using the tie beam to change the effective length of the restraining tubes or by using tubes of different wall thickness. The internal diameters of the Tee pieces were machined to allow a sliding fit for the test pieces.

Location plattens provided work surfaces on which the T-pieces could be fixed at the appropriate spans. These plattens were rigidly fixed to support beams which in turn were anchored to the laboratory floor.

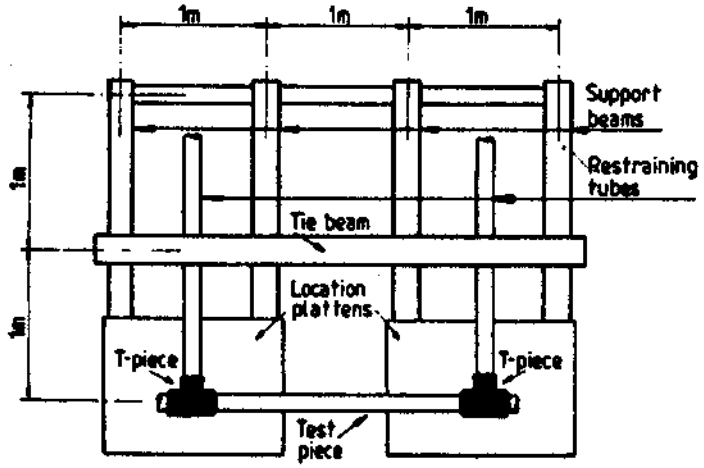

Figure 9
Tube support frame

3.1.2 Loading rig

The Dartec test machine in the Heavy Structures Laboratory at the University of Strathclyde allowed the specified stroke rate and maximum stroke to be achieved but the capacity of the available jack was 250 kN. A scissors system, lying in a horizontal plane, was devised to increase this maximum to 1000 kN. Details of this system are shown in Figure 10.

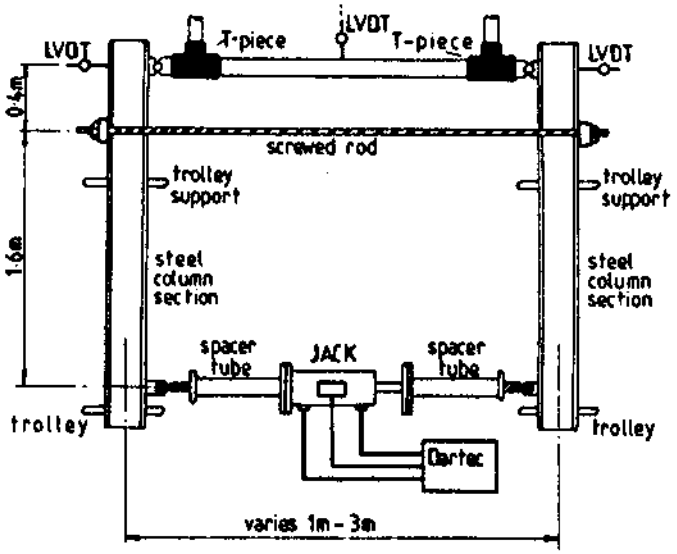

Figure 10
Scissors arrangement

The force from the Dartec 250 kN hydraulic jack was transferred to the test piece by Universal Column sections. These sections were arranged to pivot about a high tensile steel rod which divided their lengths in the ratio of 4:1. The different lengths of test piece were accomodated by bolting steel spacer tubes onto the ends of the jack. At the ends of the spacer tubes a ball and socket arrangement eliminated any bending action between the spacer tubes and the columns.

Steel plugs were turned to fit tightly inside the ends of the test pieces. The plugs were bolted to round steel bars of diameter equal to that of the external diameter of the test pieces. These bars formed the bearings on one side of a fulcrum arrangement. The other side of the fulcrum was formed by welding similar steel bars to the face of the scissor beams, matching semi-circles from each bar and inserting steel pins between the bars.

The weight of the scissors arrangement was carried by two trolleys, one under each beam, with nylon castor wheels with nylon bearings. A third trolley was placed immediately adjacent to the Dartec jack. This arrangement allowed the scissors arrangement to move laterally to take up an equilibrium position with a minimum of frictional resistance.

3.1.4 Instrumentation

Load was obtained by monitoring voltage output from the control panel of the Dartec testing machine. Throughout the test the load-deflection (of the jack) resonse was displayed on the Dartec pen recorder. While exact values could not be obtained from this graph it gave a useful indication of the progress of the test.

Linear Variable Displacement Transducers (LVDT) were used to measure the transverse deflection of the tension face behind the dent at the centre of the test piece and the axial deflection at both ends.

Strain was measured at the positions shown in Figure 11. These were the same gauges as were used in the dynamic tests. Before testing the gauges were examined and

were monitored directly using a micro-computer using a programme which was specifically written for the purpose. Additionally, all signals were continuously recorded on a Racal Store 14DS instrumentation tape recorder. In this way what were essentially sacrificial tests became available for repeated scrutiny.

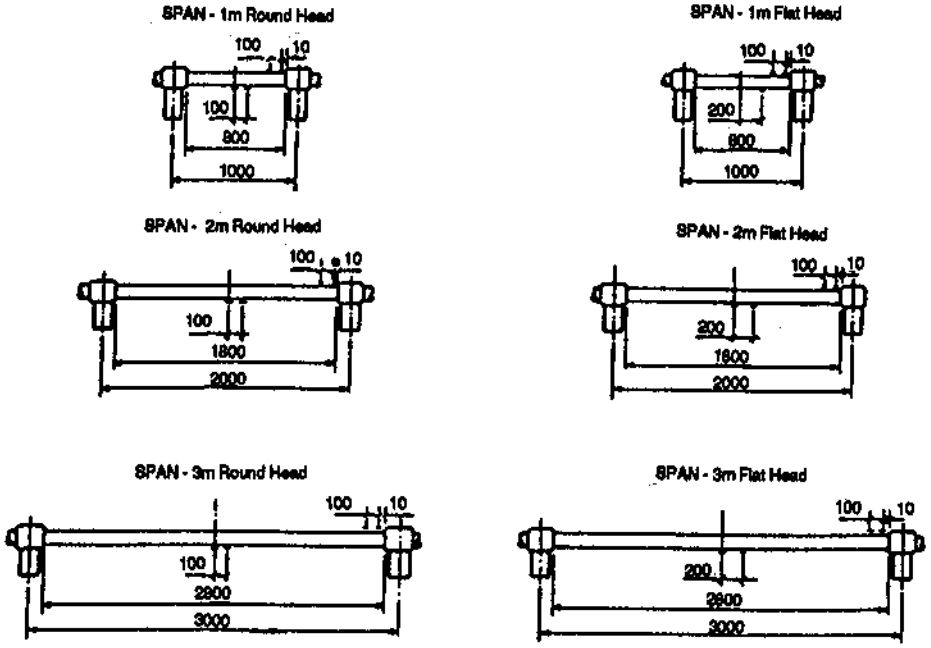

Figure 11
Arrangement of strain gauges

3.2 PROCEDURE

3.2.1 General

The Tee-pieces, the end plugs and the ends of the test specimens were greased before the test piece was positioned and the end restraints fitted. The LVDTs were then positioned and the bridges to the strain gauges balanced. The Dartec test machine was set to zero load and these initial conditions were recorded.

3.2.2 Load application

The Dartec settings were put on stroke control and adjusted to give a rate of strain in the test piece of approximately 20μstrain/sec. The strain rate at the test specimen was generally less than the stroke rate of the jack due to straining in the loading rig. This reduction in axial strain rate was greatest during the initial loading when the axial stiffness of the test piece was greatest. As the specimen reached the condition of continuing strain under constant load the strain rate was closest to 20μstrain/sec.

All specimens were strained until an axial deormation of 40 mm had been achieved or until the load had reduced considerably during continuously increasing strain. Thereafter the load was reduced to zero under constant strain rate.

3.3 RESULTS

3.3.1 General

Typical results for tests using the round impactor on a thin walled tube and on a thick walled tube are shown graphically in Figure 12 and Figure 13. Variations of transverse deflection, axial deflection and micro-strain are plotted against load. The maximum theoretical load (as derived later) is indicated on the graph of load against transverse deflection. A straight line from the origin of the load against strain graphs, denoting P/AE, represents the nominal load-strain relationship of the tube with full cross-section, no dent and no out of straight.

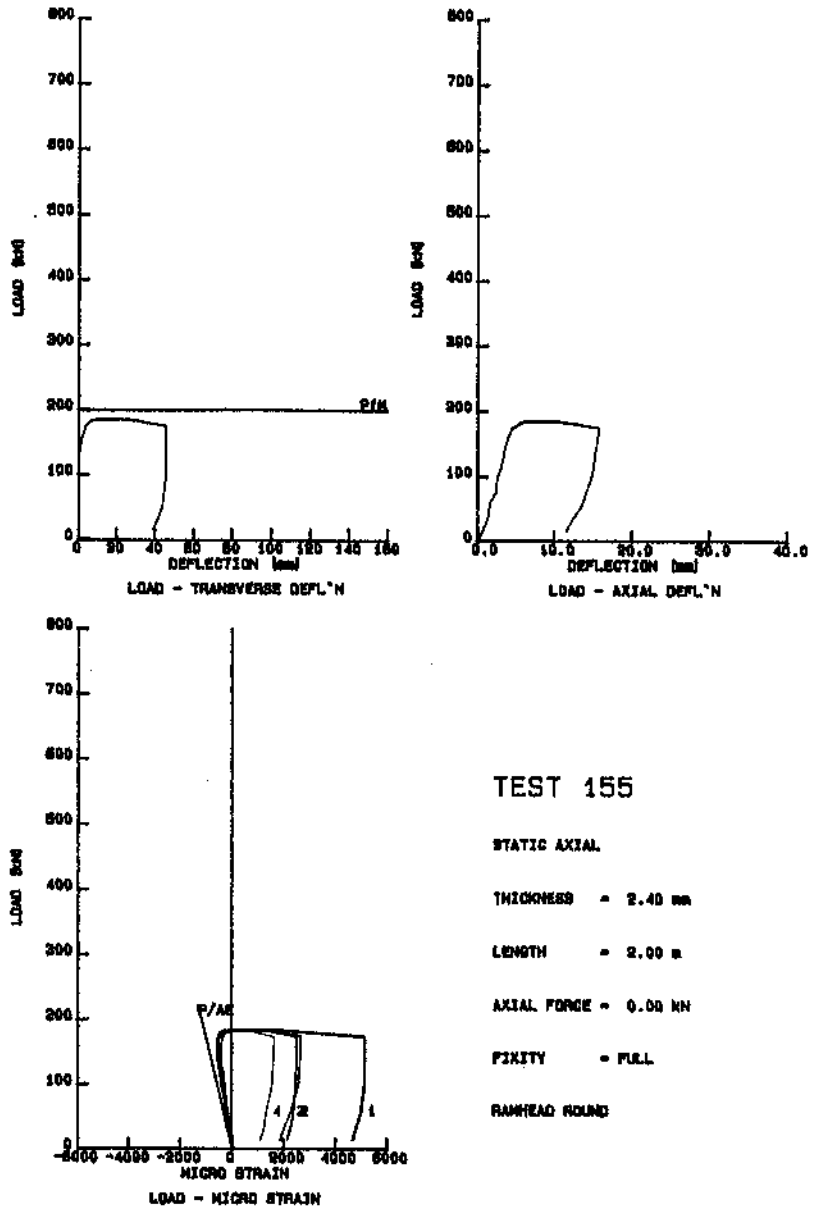

Figure 12
Results for typical thin walled tube

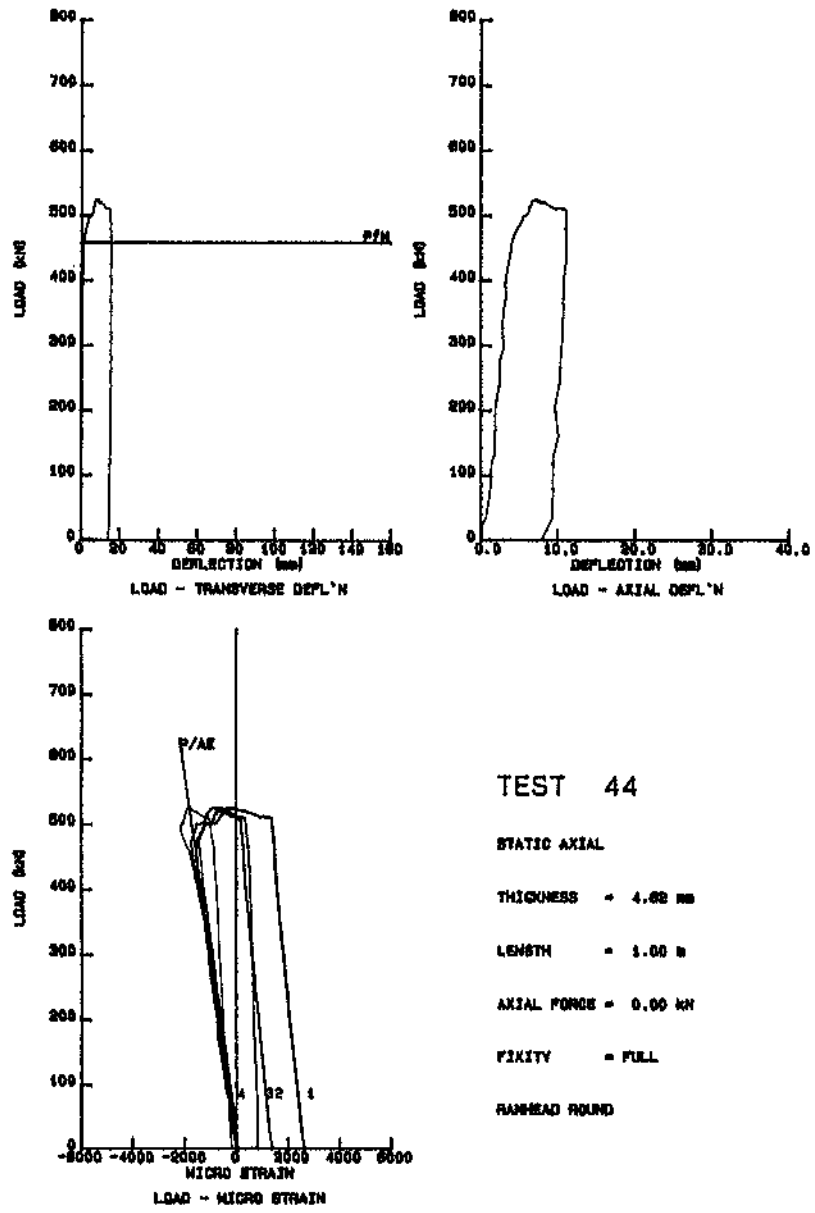

Figure 13
Results for typical thick walled tube

A table of numerical results is given in Appendix B. This table lists the maximum experimental load achieved. Experimental elastic strain and axial stiffness have been calculated from the straight line between the origin and a load value of 50% of maximum load. The theoretical values are based on straight tubes with no dent. The comparison between experimental and nominal strain is based on the average strain recorded at Gauges 1 and 2.

3.3.2 Axial stiffness

The table in Appendix B indicates a broad agreement for the axial stiffness within groups of similar tubes. While two tests appear to be faulty, Nos 62 and 67, most inconsistencies are associated with the flat ram impactor. A summary of the relationship between experimental and nominal theoretical axial stiffness is shown in Figure 14. In this graph the theoretical axial stiffness has been taken to be PL/AE.

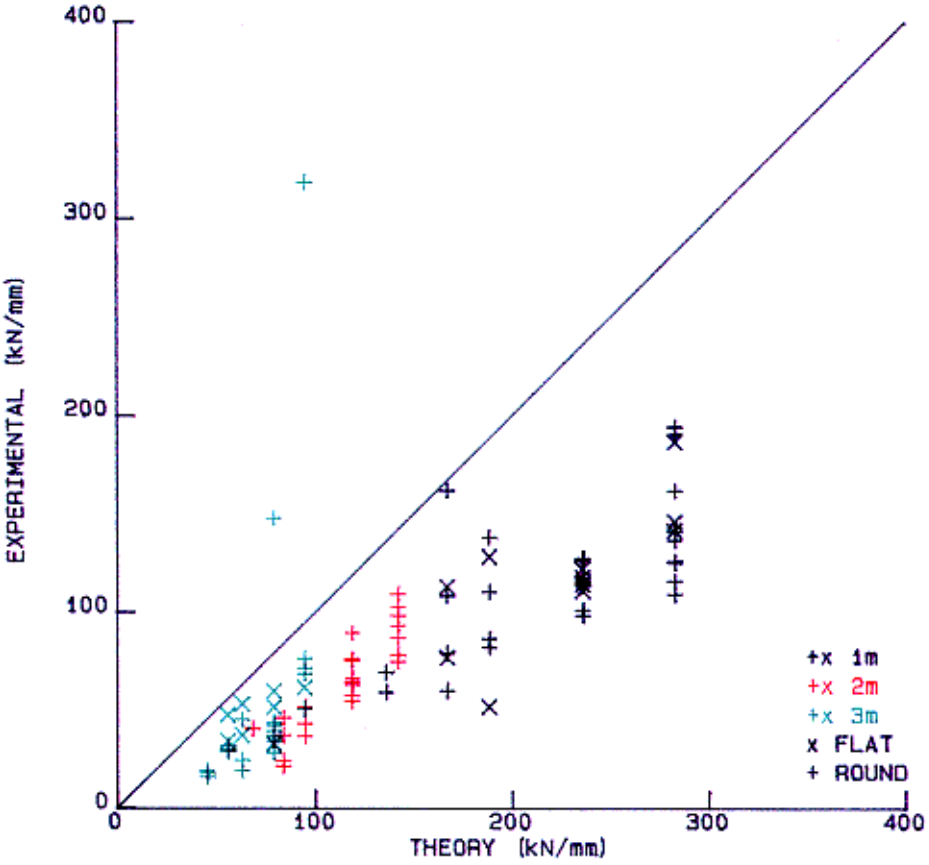

Figure 14
Axial stiffness

The presence of residual deflection or a dent will reduce the axial stiffness and consequently all points should lie below the equality line. This is mainly so; the major exceptions being Tests 62 and 107 for which no explanation can be found. A crude approximation is that the tubes have lost about 50% of their axial stiffness as a consequence of both dent and residual deflection.

3.3.3 Transverse deflection

The table of results for the transverse deflections shows little correlation between groups of similar tubes. In a significant number of cases there was little or no measurable deflection for a large part of the loading range. Apart from this cursory survey, these results have not been considered further.

3.3.4 Axial strain

Figure 15 summarises the comparison between experimental and nominal theoretical strain

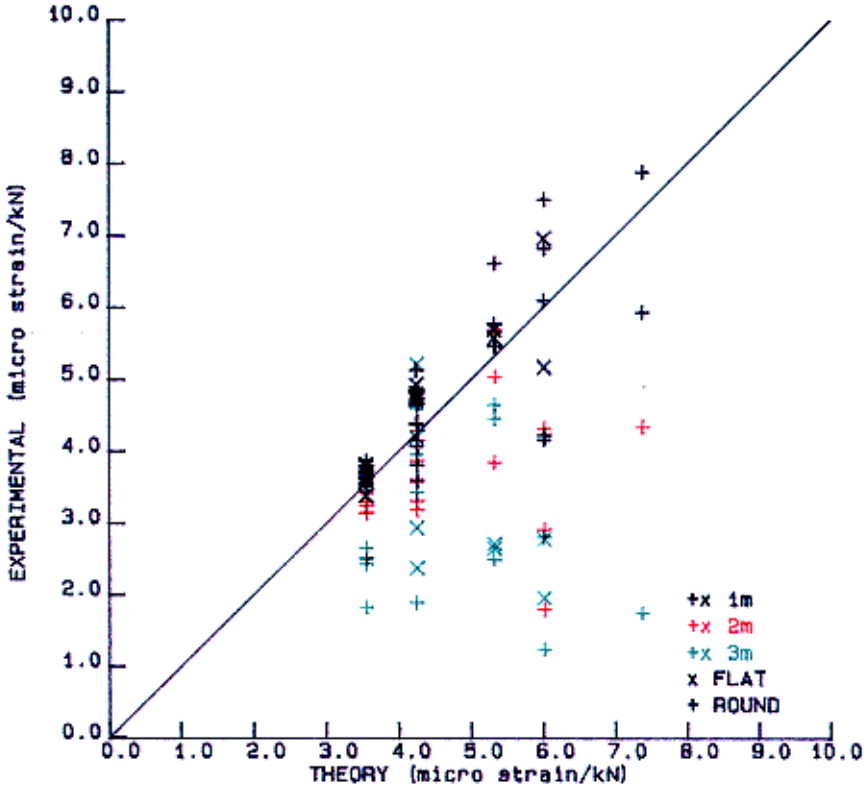

Figure 15
Axial strain

The points in this graph lie along vertical lines corresponding to each tube thickness, with the thinner tubes having higher strain per load. It can be seen that the thinner the tube the greater the scatter of points along a line. Further, the longer the tube, the greater is the difference between theory and experiment. The longer tubes are more flexible in bending and produce higher bending strains adjacent to the support. The short thin tubes have the greater dents. These consequently have a high effect on the overall eccentricity of the tube geometry which leads to higher bending stresses in the vicinity of the support.

3.4 CONCLUSIONS

The test apparatus performed well. A comparison of results among specimens in similar groups shows similar results with few exceptions.

The simple comparisons of axial stiffness and strain with the corresponding nominal theoretical values appear to follow the expected trend. Inconsistencies in axial stiffness were generally not corroberated by the strain results. Also inconsistent strain results were not substantiated by the corresponding axial stiffness.

The method of assessing the estimated linear behaviour could lead to erratic results. A study of the test results for axial deflection and strain shows that the variations were not necessarily consistent. The small deviations fom a smooth curve were sometimes significant and could affect the linear calculations. More consistent results might be obtained from an individual manual examination of each test.

4. THEORETICAL ANALYSIS

4.1 LITERATURE REVIEW

Ellinas and Walker [2] reviewed publications on the analyses of the strength of damaged tubulars. Some of these analyses were highly sophisticated and based on elastic-plastic finite element analyses [3-7]. Such analyses are expensive and tend to be restricted to specific parameters. Although having a high degree of accuracy, they are not suitable for general application. Furthermore, the combined effects of damage and residual deflection with various end restraints have not been adequately covered.

The work most relevant to this study is that described by Ellinas [8] in which the effects of the dent and residual deflection are considered. This leads to an expression for the average axial stress at failure which has a form similar to the Perry-Robertson solution for the strength of struts. The analysis of the plastic moment of resistance of the dented section is based on the approximate section shown in Figure 16. This analysis gives consistently conservative results when compared with a range of test results from various sources; all tests lying within the range $30 < D/t < 90$.

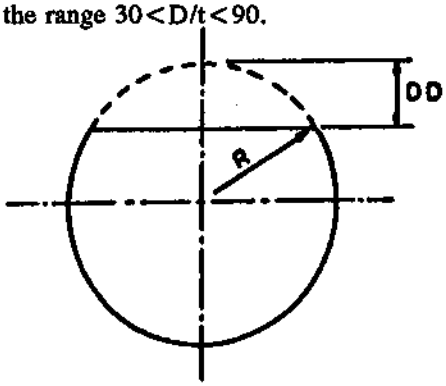

Figure 16
The Ellinas dent

4.2 APPROXIMATE PLASTIC MOMENT OF RESISTANCE OF DENT

When the test piece had been loaded to failure, a study of the dent profiles and the deformed cross section showed that, generally, the flat portion of the dent (AA in Figure 17), together with a short length below AB, had buckled.

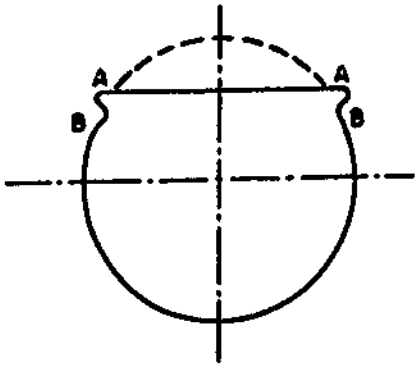

Figure 17
Approximate dent profile

As a first approximation, only that arc bounded by AA in Figure 17 was considered when considering the elastic-plastic behaviour of the dented section under the action of combined action of axial and bending forces. Referring to Figure 18:

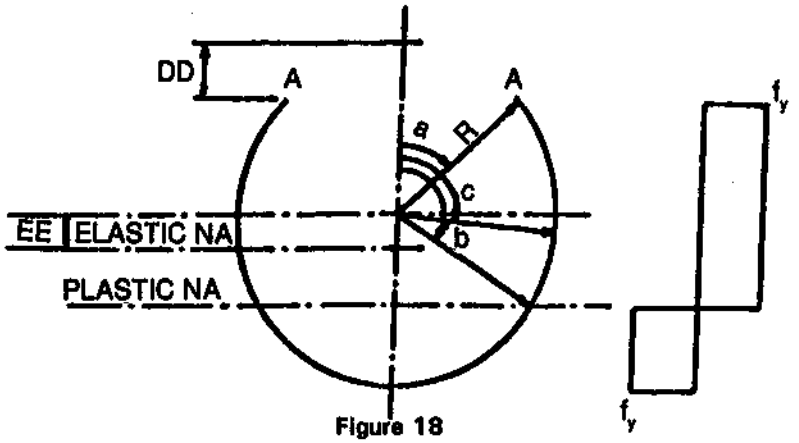

Figure 18
Analytical section

the angle, a, is given by:

$$a = \cos^{-1}\left[\frac{(R-DD)}{R}\right] \qquad \text{Eqn 3}$$

The plastic neutral axis is located at an angle "b". This is obtained by integrating the stress on either side of the neutral axis and equating to the axial force:

$$P = 2RTf_y\,[(b-a) - (\pi - b)] \qquad \text{Eqn 4}$$

The arc length considered to sustain the axial force, P, is that between the angles "c" and "b". The angle "c" is obtained from:

$$c = b - \frac{P}{2RTf_y} \qquad \text{Eqn 5}$$

The reduced plastic moment of resistance is found by integrating the moment from the stress about the plastic neutral axis:

$$\begin{aligned} M_{pr} &= 2R^2Tf_y[\textstyle\int_a^c \cos i.di - \int_0^b \cos i.di] \\ &= 2R^2TF_y[\sin c - \sin a + \sin b] \end{aligned} \qquad \text{Eqn 6}$$

4.3 ANALYSIS OF THE SYSTEM

The simple beam system shown in Figure 19 was used as the basis of the analysis.

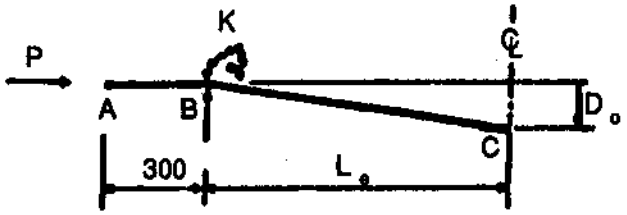

Figure 19
Idealised geometry

The support at B represents the T-piece in the tests where lateral movement was prevented and various degrees of rotational restraint were imposed. The dimension, D_o, was taken as the sum of the residual deflections obtained from the dynamic tests and the eccentricity, EE, of the elastic neutral axis of the equivalent arc. From Figure 18, EE is defined from:

$$EE = \frac{R\sin.a}{-a} \qquad \text{Eqn 7}$$

The length, L_e shown in Figure 18, is half the nominal span for specimens tested using the round indenter. Where the flat indenter was used L_e is the distance of the maximum dent from the support. The projection AB represents the projection from the T-piece to the hinge on the test specimen. This varied slightly but was typically of the order of 300 mm. This parameter was included as the rotation of the T-piece gave rise to an added moment during the loading of the specimen.

The rotational stiffness, K, was that calculated from the size and length of the restraining leg for a particular test.

A plane frame analysis which incorporated Livesley's stability functions (9) was carried out. The elastic properties of the elements AB and BC were taken as those of the full circular section. The reduced plastic moment of resistance at C was that for the dented section derived in part 4.2. The corresponding reduced plastic moment at B, on BC, was the standard expression for a circular hollow section. The steps in the analysis were as follows:

- Initially a boundary condition of zero slope was applied at C. By a process of iteration the axial force, P, was adjusted until the moment at C was equal to the plastic moment of resistance for that axial force. This defined the force, P1, for the first hinge at C.
- The load was then stepped in increments of (PY - P1)/50, where PY is the squash load for the full section. During these load increments, zero rotational restraint was imposed at C but the reduced plastic moment of resistance for the particular axial load was applied. This necessitated some iteration at each increment to achieve the correct balance. The maximum load carrying capacity was then defined by one of the following criteria.
- If the reduced plastic moment of resistance at C was approximately zero then the specimen was deemed to have failed by axial squashing at C. This type of failure is denoted by 'S' in the reported results.
- If the reduced plastic moment of resistance of the full section at B on BC was reached then the specimen was deemed to have failed by a bending mechanism. This type of failure is denoted by 'M' in the reported results.
- If the determinant of the structural stiffness matrix was less than, or equal to, zero then the system had become unstable. This type of failure is denoted by 'U' in the reported results.

4.4 ANALYTICAL RESULTS

The results of the analysis of each test are tabulated in Appendix C. The table compares the theoretical results with experimental, using the former as the base for the comparison. This comparison is summarised in Figure 20. Generally there is good agreement with most of the experimental results lying within 20% of the theoretical. The trend is, however, for the theoretical analysis to under estimate the maximum force at lower values of the force and to over estimate it at higher values.

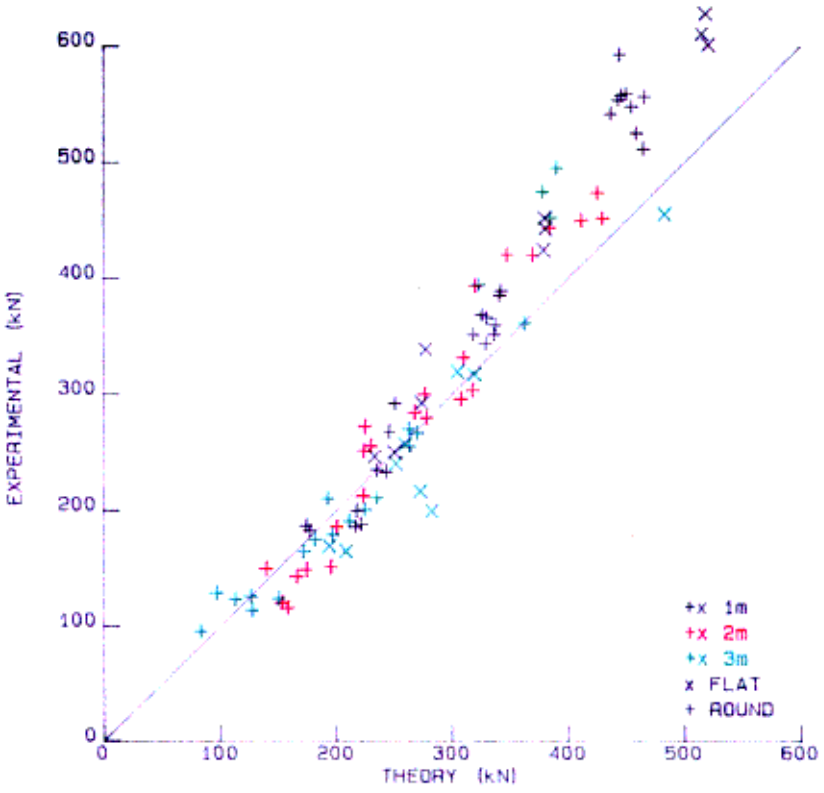

Figure 20
Maximum force

The higher experimental loads occur in the tubes with the thicker wall thicknesses and with small dents. The assumption made in the theoretical analysis that the dented area is ineffective is over conservative. A re-analysis of these sections, using the equivalent section shown in Figure 21 brought the theoretical results close to the those obtained experimentally.

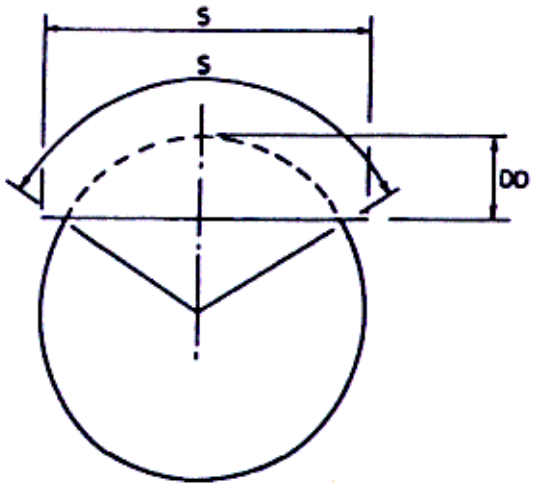

Figure 21
idealised conservative dent

The lower experimental loads occur in the thinner walled tubes with larger dents. In these cases a larger part of the dented area buckled out than was assumd in the theoretical analysis (AB in Figure 17).

The results for the dents created by the flat ram are not in greater error than those from the round ram. However the theoretical maximum loads for those specimens which had been subjected to the flat ram differed significantly from the experimental; this error being due to the neglect of the length of dent within the plate.

The ratio of theoretical to experimental failure load is plotted against the dimensionless parameter 'Residual deflection over span' in Figure 22, against 'Dent depth over thickness' in Figure 23, and against 'Dent depth over diameter' in Figure 24.

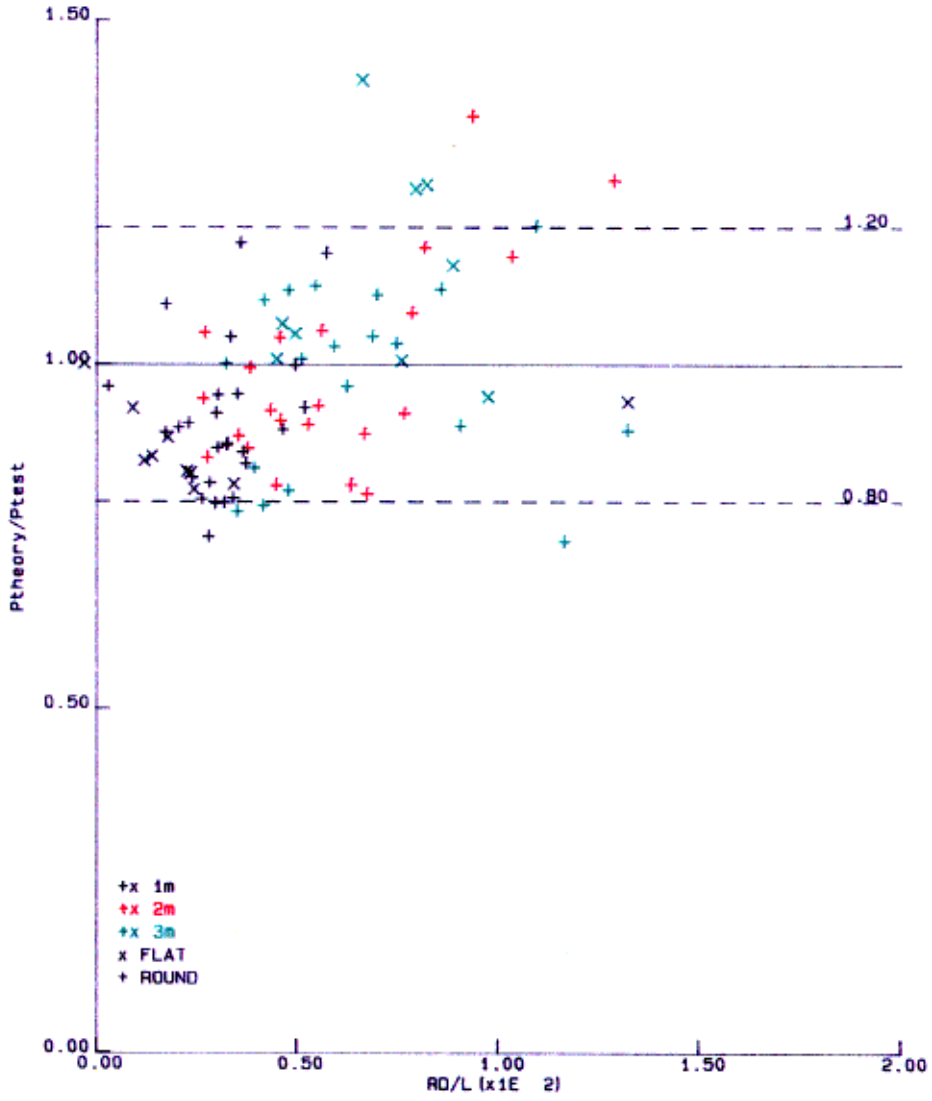

Figure 22
Relationship of maximum load to residual deflection

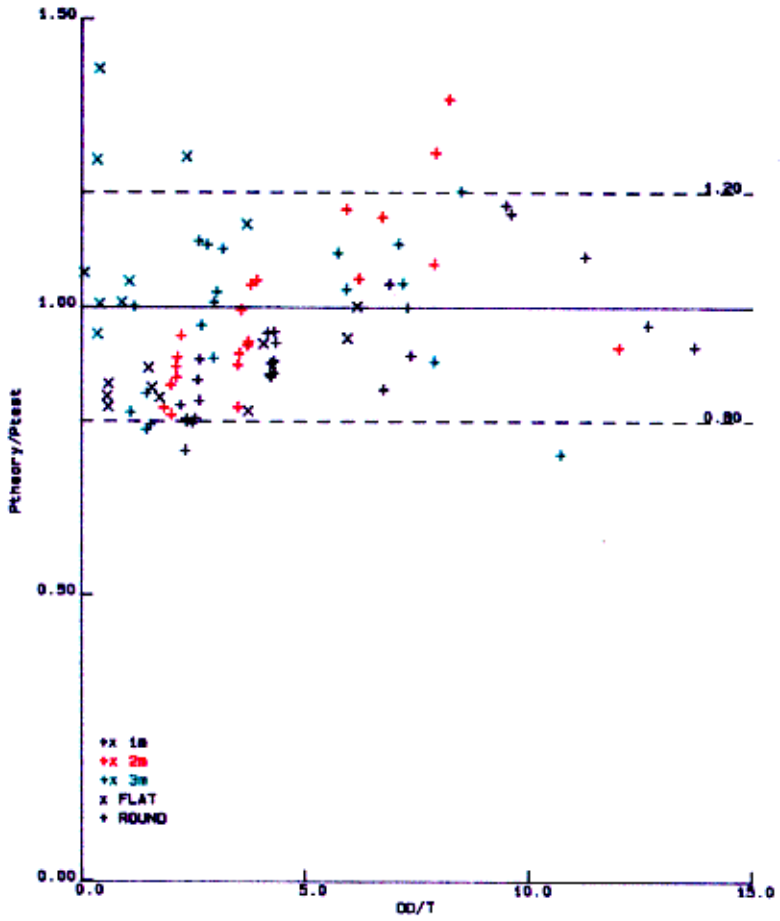

Figure 23
Relationship of maximum load to dent depth and wall thickness

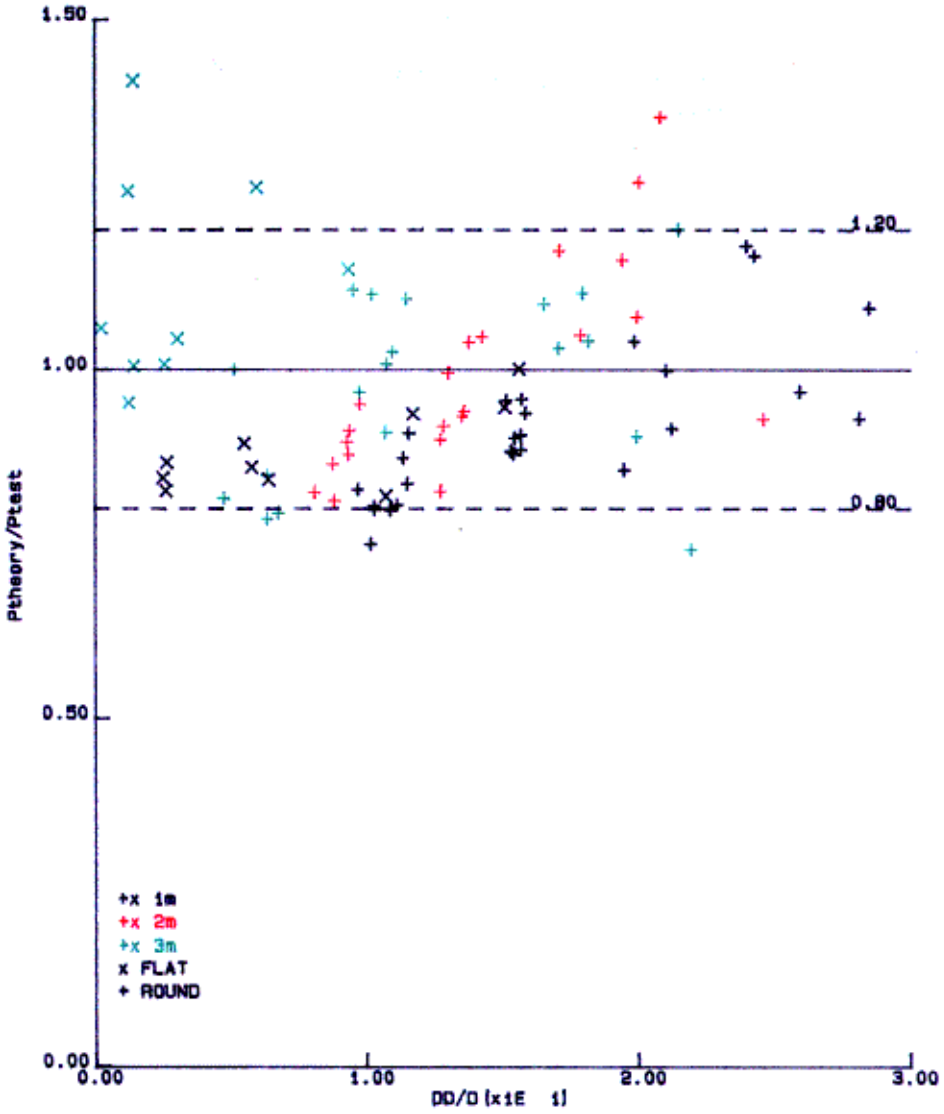

Figure 24
Relationship of maximum load to dent depth and diameter.

Figures 22, 23 and 24 display those sections in which theoretical and experimenta results differ by more than 20%. In two tests using the round indentor (Test Nos 156 and 157) the theoretical maximum force excedes the experimental. Both of these tests involved tubes of 2.58 mm wall thickness spanning 2 m with large dents. The results of the dynamic tests on these specimens were consistent within their group.

Test numbers 182 and 183 involved tubes of 2.09 mm wall thickness with spans of 3 m. In test 182 the theoretical maximum load was 75% of that achieved experimentally: in test 183 it was 30% lower than that. No explanation has been found for these a-typical results.

Test numbers 126, 127 and 168 all involved 3 m spans: the wall thickness of the tubes in tests 126 and 127 being 3.7 mm that in test 168 being 2.58 mm thick. The flat indentor was used in all three tests. The results for tests 126 and 127 are similar with the theoretically calculated maximum load significantly less than that obtained experimentally. The results of test 168 can be compared with those for test 169. The difference in maximum load is most probably due to the differences in the geometry of their dents.

All of the parameters considered are interdependent and cannot be considered in isolation. Figures 22,23 and 24 show potential trends which may be useful in further studies to refine the theory presented.

The table in Appendix C also gives the theoretical results for two cases:

- dent only with no residual deflection
- nominal residual deflection only

These solutions are presented to give an indication of the relative effects of the dent and the residual deflection on load carrying capacity.

5. DISCUSSION

5.1 PROFILING

The dent depth, from both round and flat indentors, has been shown to be virtually independent of either the axial preload, applied during the dynamic tests, or the end restraint conditions; the same restraints being applied for both dynamic tests and for the static load tests. The primary factors which governed the behaviour of the specimens were wall thickness and span. For the same energy input, the resulting dent depth is inversely proportional to the span. This demonstrates that for increasing span more energy is dissipated in the elastic bending of the tube and less in dent formation

The limited number of specimens tested with the flat indentor illustrated the effect of the shape of the indentor. In these cases the dent formation made it difficult to define a dent depth as the maximum dent was not always at the centre of the impactor but rather at its edges. The dent depths were considerably smaller than those from the round indentor due th the greater spread of the impact force but the extent of cross sectional deformation was much greater.

The three dimensional nature of the dent shape has not been analysed. This could be used to verify sophisticated analyses based on the elasto-plastic material properties.

The measured dent depths were experimentally consistent. The results from the round indentor bore little relationship to estimated values derived from a study of dents produced by static loading although there were similarities in profiles. Generally, the experimental length of the dent varied linearly with dent depth while the length calculated theoretically assumed that the length was only a constant function of the diameter for a given depth.

The calculation of dent volume was unsatisfactory. The volume change is small relative to total volume and it is propable that the simple integration techniques were insufficiently refined numerically. A more detailed study of dent shape along with more sophisticated numerical methods may lead to more meaningful results.

The specimens from the static bending tests of the first study were not profiled. The comparison of dent lengths with those produced by others from static tests had a poor correlation. Here is potential for an investigation into the relationship between dents produced statically and dynamically, both resulting from the same energy input. Axial load tests on specimens with significant differences in dent profiles would yield more information on the influence of dent shape on residual axial load carrying capacity.

5.2 COMPARISON WITH RESULTS FROM DYNAMIC TESTS

One of the important consequences of profiling was that it allowed an assessment of the validity of the dynamic test results through a comparison of dent depth. The calculation of dent depth from dynamic tests involved the main instrumentation of velocity, load and deflection. The generally good correlation in the tests involving the round indentor demonstrates the accuracy of the dynamic results. The results from tests involving the flat indentor do not compare well. This is due to the method of measuring dent depth from dynamic results which related only to the dynamic behaviour of the indentor as a whole. No account was taken of the complicated dent shape and cross sectional deformation which was actually produced. It is doubtful if there is any single method of accurately measuring the dent from such an indentor under dynamic conditions.

Information is now available to relate dent characteristics to energy input. Such analyses are not included in this report.

5.3 AXIAL TESTS

Satisfactory results were obtained from the axial tests and the apparatus performed consistently well. The tests showed that the effect of the dent in conjunction with residual deflection was to reduce both the maximum load and axial stiffness. Generally the reduction was of the order of 20%-50% but for some thinner tubes with large dents reductions in excess of 50% were found. This reduction in stiffness might significantly effect the stability of the whole structure.

5.4 THEORETICAL ANALYSIS

The theoretical analysis was derived with the object of producing an analysis which was:

- simple
- capable of being programmed for use on a micro computer
- took account of all major parameters
- produced reasonably accurate results

These aims have been satisfied. The analysis generally predicts results to within 20% of those obtained experimentally. This is true for both round and flat indentors. Considering variations in material properties, section geometry,dent profile, end restraints together with experimental error, this degree of accuracy is considered to be satisfactory. However, the error in the theoretical analysis does have a trend in that the theory underestimates the axial load capacity when the dnt is small and overestimates capacity for large dents. This is due to an over simplistic approach to the plastic behaviour of the dented section.

The analysis is capable of predicting strain in the tube. This option has not been pursued but a comparison of theoretical and experimental strains adjacent to the supports would be valuable as a further assessment of the validity of the analysis. A study of theoretical and experimental axial stiffness would serve the same purpose.

It has been shown that the analysis can be improved, by the inclusion of an empirical parameter, to control the effective dent width. The analysis of tubes dented by the flat indentor can also be improved by including an additional element over the length between the sections at which the maximum dents occur. While the local rigidity of the T-piece has also been ignored, it is felt that any loss of accuracy due to this will be of minor significance.

Both the tests and the analuses have only considered the situation where the dent occurs at the centre of the span. The analyses are easily modified to encompass the complete span and to cover the likely practical cases of unsymmetrically located dents. In view of the accuracy in the symmetrical analyses it is reasonable to assume that this accuracy will be maintained the analyses are extended to include unsymmetrical cases.

In practce, situations might occur which would give rise to biaxial bending in the tubes. This is a much more complex situation and, while the analysis can be modified to include such conditions, the accuracy of any solution would require to be verified by testing.

A comparison of the theoretical and experimental results with those derived by Ellinas might be worthwhile. The Ellinas approach has the advantage of simplicity but it is felt that its application may be restricted by the form of the dent profile assumed.

6. GENERAL CONCLUSIONS

A large number of tubular specimens have been tested under impact loading and thereafter under static axial loading. The dents from impact have been profiled and the damaged tubes have been tested under axial compressive load to failure. Theories have been developed to estimate the reduction in load carrying capacity of the damaged tubular. The approximate analyses developed have produced results which compare with the experiments measured.

The test programme described in OTI 88 532 together with the work described here have produced a large amount of data. This experimental database will be used by the HSE to validate theoretical models in the subject area.

To date, the studies on the effects of impact on tubulars have been restricted to a consideration of isolated members. The effects of such damaged members on the total behaviour of the structure also needs investigation. There is the possibility that the damaged test specimens from this programme could be used in a further programme to assess the efficiency of repair techniques on damaged members, with especial emphasis on further impact.

REFERENCES

1. **ALLAN, J D and MARSHALL J**
   Ship impact on steel tubulars
   Offshore Technology Report No OTI 88 532, HMSO, 1988

2. **ELLINAS, C P and WALKER, A C**
   Damage on offshore tubular bracing members
   IABSE Colloquium, Copenhagen, 1983

3. **SMITH, C S, KIRKWOOD, W and SWAN, J W**
   Buckling strength and post-collapse behaviour of tubular bracing members including damage effects
   Boss"79, Imperial College, London, 1979

4. **SMITH, C S, SOMERVILLE, W L and SWAN, J W**
   Residual strength and stiffness of damaged steel bracing members
   Offshore Technology Conference, Paper No OTC 3981, Houston, 1981

5. **MOAN, T and TABY J**
   Theoretical and experimental study of the behaviour of damaged tubulars in offshore structures
   Norwegian Maritime Research, No 2, 1981

6. **de OLIVEIRA, J G**
   Design of steel offshore structures against impact loads due to dropped objects
   International Symposium on Offshore Engineering, Rio de Janeiro, 1981

7. **de OLIVEIRA, J G**
   The behaviour of steel offshore structures under accidential collisions
   Offshore Technology Conference, Paper No OTC4136, Houston, 1981

8. **ELLINAS, C P**
   Ultimate strength of damaged tubular bracing members
   American Society of Civil Engineers, Journal of the Structural Division, February, 1984

9. **LIVESLEY, R K**
   Matrix methods in structural engineering
   Pergammon Press, 1964

APPENDIX A

TABLE OF PROFILING RESULTS

NOTES:

The terms used in this appendix have the following meanings:

DEPTH	Dent depth.
LENGTH	Dent length defined by 5% of dent depth.
VOLUME	Dent volume.
R	Round impactor.
F	Flat impactor.
Pr	Results from profiling.
DYN	Results from dynamic tests.
%	(DYN-Pr)*100/Pr
Pr/Th	(LENGTH)/(LENGTH from Eq.1 at 5% dent depth)
***	Results from dynamic tests not available.

TEST	T mm	L m	DEPTH mm			LENGTH mm		VOLUME
			Pr	DYN	%	Pr	Pr/Th	mm³/1E4
44R	4.46	1.0	11.53	11.75	2	148	0.6	0.95
45R	4.46	1.0	11.76	12.47	6	156	0.7	2.26
46R	4.46	1.0	11.70	8.27	-29	162	0.7	1.91
47R	4.46	1.0	9.84	7.49	-24	120	0.5	1.50
48R	4.46	1.0	11.08	8.57	-23	148	0.6	1.12
49R	4.46	1.0	10.45	8.25	-21	163	0.7	1.79
50R	4.46	1.0	10.47	7.63	-27	135	0.6	1.58
51R	4.46	1.0	10.33	7.49	-28	153	0.7	2.28
52R	4.46	1.0	11.35	10.07	-11	155	0.7	1.19
53R	4.46	2.0	9.51	7.97	-16	152	0.6	1.39
54R	4.46	2.0	9.91	7.08	-29	149	0.6	0.94
55R	4.46	2.0	9.41	6.49	-31	154	0.7	1.91
56R	4.46	2.0	8.87	9.80	11	159	0.7	1.20
58R	4.46	2.0	9.48	9.67	2	146	0.6	1.99
59R	4.46	2.0	8.18	8.52	4	146	0.6	1.19
61R	4.46	2.0	8.95	9.56	7	142	0.6	1.06
62R	4.46	3.0	6.41	8.63	35	129	0.5	0.78
63R	4.46	3.0	6.41	6.20	-3	132	0.6	1.97
64R	4.46	3.0	6.84	4.51	-34	135	0.6	1.49
65R	4.46	3.0	5.18	5.93	14	137	0.6	1.34
70R	4.46	3.0	4.80	8.89	85	139	0.6	2.56
78F	4.46	1.0	2.67	3.26	22	276	1.2	1.48
79F	4.46	1.0	2.71	2.42	-11	304	1.3	1.46
80F	4.46	1.0	2.55	4.23	66	353	1.5	1.48
82F	4.46	3.0	0.23	-4.60	***	201	0.9	2.60
87R	3.70	1.0	16.12	14.30	-11	180	0.8	2.80
88R	3.70	1.0	15.93	13.35	-16	191	0.8	2.14
89R	3.70	1.0	15.66	12.37	-21	190	0.8	1.42
90R	3.70	1.0	15.38	13.07	-15	171	0.7	1.36
91R	3.70	1.0	15.97	19.09	20	185	0.8	2.05
92R	3.70	1.0	15.56	*****	***	181	0.8	1.50
93R	3.70	1.0	15.55	10.81	-31	186	0.8	1.70
94R	3.70	1.0	15.71	14.30	-9	182	0.8	2.70
95R	3.70	1.0	15.93	14.25	-11	179	0.8	1.55
96R	3.70	2.0	14.46	20.54	42	176	0.8	1.40
97R	3.70	2.0	13.70	11.93	-13	179	0.8	1.98
98R	3.70	2.0	13.98	11.94	-15	173	0.7	2.07
99R	3.70	2.0	13.00	10.98	-15	165	0.7	1.68
100R	3.70	2.0	13.79	13.94	1	176	0.8	2.35
101R	3.70	2.0	13.18	10.57	-20	178	0.8	2.23
102R	3.70	2.0	12.88	11.26	-13	161	0.7	1.54
103R	3.70	2.0	12.88	10.61	-18	156	0.7	1.65
105R	3.70	3.0	10.90	20.98	93	135	0.6	1.11
106R	3.70	3.0	11.15	10.95	-2	146	0.6	1.62
107R	3.70	3.0	9.86	9.19	-7	89	0.4	-1.81
108R	3.70	3.0	10.36	9.77	-6	214	0.9	5.91
110R	3.70	3.0	11.67	13.78	18	144	0.6	0.99
111R	3.70	3.0	9.63	11.64	21	147	0.6	1.02
113R	3.70	3.0	10.87	11.09	2	145	0.6	0.85

TEST	T mm	L m	DEPTH mm			LENGTH mm		VOLUME
			Pr	DYN	%	Pr	Pr/Th	$mm^3/1E4$
120F	3.70	1.0	6.11	*****	**	351	1.5	0.52
121F	3.70	1.0	6.47	6.90	7	385	1.6	2.32
122F	3.70	1.0	5.85	5.58	-5	363	1.6	2.76
123F	3.70	1.0	5.57	1.11	-80	319	1.4	2.38
124F	3.70	3.0	1.26	-1.72	**	270	1.2	1.05
125F	3.70	3.0	1.47	-4.35	**	277	1.2	2.10
126F	3.70	3.0	1.44	4.04	180	288	1.2	1.48
127F	3.70	3.0	1.24	5.34	331	267	1.1	1.36
130R	2.93	1.0	19.81	18.48	-7	210	0.9	1.84
131R	2.93	1.0	21.57	18.37	-15	214	0.9	2.64
132R	2.93	1.0	20.17	19.51	-3	216	0.9	1.84
133R	2.93	1.0	21.37	20.23	-5	204	0.9	2.31
135R	2.93	2.0	18.12	15.51	-14	170	0.7	0.57
136R	2.93	2.0	17.33	21.07	22	162	0.7	0.52
137R	2.93	2.0	19.72	17.09	-13	194	0.8	2.81
138R	2.93	3.0	16.76	26.63	59	163	0.7	1.11
139R	2.93	3.0	17.33	19.25	11	169	0.7	1.39
141R	2.93	3.0	15.80	16.94	7	158	0.7	1.41
145F	2.93	1.0	10.88	11.89	9	375	1.6	2.62
146F	2.93	1.0	11.91	11.45	-4	381	1.6	3.23
147F	2.93	3.0	2.60	16.32	528	373	1.6	1.95
148F	2.93	3.0	3.10	10.82	249	371	1.6	1.37
151R	2.58	1.0	23.69	*****	**	220	0.9	2.64
152R	2.58	1.0	29.04	28.61	-2	241	1.0	4.41
153R	2.58	1.0	24.42	22.70	-7	221	0.9	2.44
154R	2.58	1..0	24.75	*****	**	226	1.0	1.37
155R	2.58	2.0	20.27	21.16	4	176	0.8	0.38
157R	2.58	2.0	21.17	25.18	19	171	0.7	0.23
158R	2.58	2.0	20.36	25.57	26	169	0.7	0.24
159R	2.58	3.0	18.49	20.47	11	185	0.8	2.35
160R	2.58	3.0	21.88	25.93	19	185	0.8	0.51
161R	2.58	3.0	18.23	20.80	14	175	0.7	1.02
162R	2.58	3.0	20.29	25.92	28	166	0.7	0.87
166F	2.58	1.0	15.89	19.24	21	372	1.6	5.24
167F	2.58	1.0	15.34	-0.28	**	384	1.6	4.73
168F	2.58	3.0	6.03	40.48	571	328	1.4	-0.46
169F	2.58	3.0	9.50	8.35	-12	193	0.8	173.04
172R	2.09	1.0	26.46	28.50	8	244	1.0	2.35
175R	2.09	1.0	28.66	30.35	6	281	1.2	5.52
179R	2.09	2.0	25.04	25.49	2	232	1.0	1.10
182R	2.09	3.0	22.32	26.65	19	161	0.7	0.31

APPENDIX B

TABLE OF RESULTS FROM AXIAL TESTS

NOTES:

The terms used in this appendix have the following meanings:

Pmax	Maximum axial force.
P/Da	Axial stiffness calculated assuming a straight line variation between the third experimental reading and that closest to half the maximum force (Pmax).
P/Da %	The percentage difference between the nominal axial stiffness neglecting dent and residual deflection and the experimental, using the latter as a base.
P/Dt	Assumed linear Load-Transverse Deflection variation calculated as for P/Da.
Microstrain/P	Assumed linear Strain/Load variation calculated as for P/Da
Microstrain/P %	The percentage difference between the nominal strain load variation neglecting dent and residual deflection and the average of the experimental results from Gauges 1 and 2 calculated as for P/Da. Where there are no results for either Gauge 1 or 2 then the other was used for the comparison.
***	Indicates no measurable deflection within the load range considered for the linear calculation.
R	Indicates the round ram.
F	Indicates the flat ram.

TEST	Pmax	P/Da		P/Dt	Microstrain/P				
	kN	kN/mm	%	kN/mm	1	2	3	4	%
44R	525	125	-55	756	-3.6	-3.6	-3.2	-3.3	0
45R	511	162	-42	***	-4.0	-3.8	-2.7	-2.8	9
46R	556	109	-61	480	-3.6	-3.6	-3.0	-3.0	2
47R	549	298	5	***	-3.6	-3.6	-2.8	-2.8	0
48R	558	126	-55	592	-3.6	-3.7	-2.9	-3.0	2
49R	559	136	-51	791	-3.7	-3.7	-3.0	-2.8	3
50R	553	191	-32	***	-3.6	-3.8	-2.8	-2.9	7
51R	592	194	-31	***	-3.7	-3.7	-2.7	-2.8	4
52R	541	141	-50	550	-3.8	-3.9	-2.8	-2.8	7
53R	449	87	-38	117	-3.7	-3.7	-2.8	-2.6	5
54R	451	103	-27	266	-3.0	-3.3	-2.9	-2.7	-11
55R	473	109	-22	182	-3.3	-3.4	-2.7	-2.7	-6
56R	443	78	-44	146	-3.5	-3.3	-2.2	-2.3	-3
58R	419	93	-34	139	-3.1	-3.4	-2.4	-2.2	-8
59R	420	98	-30	126	-3.0	-3.3	-2.8	-2.7	-11
61R	393	74	-47	78	-3.6	-3.9	-2.1	-2.2	5
62R	452	319	238	315	-1.0	-2.6	-2.7	-3.2	-48
63R	495	51	-45	***	-2.6	-2.4	-2.1	-4.3	-29
64R	474	72	-23	***	-2.7	-2.7	-2.4		-24
65R	360	69	-26	67	-2.3	-2.8	-1.7	-1.6	-28
70R	394	77	-18	56	-2.2	-2.7	-2.2	-2.0	-31
78F	627	141	-50	***	-3.8	-3.9	-3.9	-3.9	7
79F	601	187	-33	***	-3.7	-3.9	-3.1	-4.6	7
80F	610	145	-48	***	-3.4	-3.4	-3.3	-3.4	-4
82F	455	62	-34	935	-3.7	-3.5	-2.5	-2.7	1
87R	359	127	-46	***	-5.0	-5.3	-3.6	-3.9	21
88R	385	113	-52	802	-3.9	-3.7	-3.2	-3.3	-10
89R	389	114	-51	***	-4.1	-4.0	-3.5	-3.5	-4
90R	351	101	-57	459	-4.7	-4.7	-4.0	-4.0	11
91R	343	116	-51	424	-4.9	-4.9	-3.5	-4.0	14
92R	358	127	-46	***	-4.6	-5.0	-3.6	-3.4	13
93R	368	98	-58	***	-4.4	-4.4	-4.1	-4.3	3
94R	365	117	-50	349	-4.8	-4.5	-3.4	-3.7	9
95R	351	126	-46	249	-4.3	-4.5	-3.7	-3.4	3
96R	302	64	-45	85	-2.9	-3.5	-2.9	-3.3	-24
97R	331	76	-35	89	-3.7	-3.5	-2.9		-15
98R	295	90	-24	62	-3.2	-4.1	-6.1	-3.9	-14
99R	296	66	-43	113	-5.0	-4.5	-2.5	-2.7	11
100R	283	57	-51	253	-3.1	-3.5	-2.7	-2.7	-21
101R	279	63	-46	73	-4.1	-3.7	-2.1	-1.9	-8
102R	271	55	-53	60	-3.9	-4.5	-2.5	-2.1	-1
103R	254	75	-36	51	-4.1	-4.5	-2.1	-2.1	1
104R	250	76	-35	37	-4.9	-4.7	-0.8	-1.2	13
105R	266	43	-45	48	-1.1	-2.7	-1.6	-1.6	-55
106R	254	40	-49	102	-4.5	-3.5	-0.4	-0.6	-6
107R	269	148	87	35		-3.4	-0.3	0.3	-18
108R	210	44	-44	10	-4.3	-5.3	2.0	1.6	13
110R	190	29	-63	10	-3.7	-5.5	3.2	3.1	8
111R	200	35	-55	9		-4.8	0.4	0.0	13
113R	209	37	-52	11		-3.6	2.2	1.9	-15

TEST	Pmax	P/Da		P/Dt	Microstrain/P				
	kN	kN/mm	%	kN/mm	1	2	3	4	%
120F	472	110	-53	***	-4.9	-4.7	-4.5	-5.6	13
121F	452	114	-51	***	-5.2	-4.7	-4.0	-4.0	16
122F	443	117	-50	***	-4.8	-4.8	-3.9	-4.7	13
123F	424	111	-53	***	-5.0	-4.6	-4.3	-4.5	12
124F	319	52	-34	48	-2.8	-3.1	-2.5	-2.3	-30
125F	316	60	-23	50	-2.0	-2.8	-2.6	-2.3	-44
126F	198	33	-58	9	-3.3	-5.1	2.7	3.1	0
127F	216	33	-57	11	-4.7	-5.7	1.6	1.8	23
130R	291	138	-26	***	-5.8	-5.8	-3.8	-4.0	8
131R	267	82	-56	119	-6.6	-6.6	-1.4	-3.5	24
132R	232	86	-54	132	-5.5	-5.5	-3.7	-3.7	2
133R	234	110	-41	113	-5.5	-5.5	-2.5	-3.0	2
135R	211	52	-45	54	-3.5	-4.2	-3.1	-3.1	-27
136R	148	43	-54	16	-4.8	-5.2	1.0	2.2	-5
137R	142	37	-60	12	-5.5	-5.9	4.7		7
138R	178	20	-68	20	-1.7	-3.2	-0.3	-1.0	-53
139R	174	46	-27	10	-4.1	-4.9	0.8	0.8	-15
140R	125	25	-60	7	-3.8	-5.5	5.5	4.7	-12
145F	338	52	-72	***	-6.1	-5.3	-5.4	-5.3	7
146F	291	128	-31	***	-5.8	-5.4	-5.8	-4.8	4
147F	256	53	-14	30	-2.4	-2.9	-1.9	-1.9	-50
148F	239	38	-40	47	-2.2	-3.2	-2.5	-2.0	-48
151R	207	108	-35	318	-6.0	-6.2	-4.7	-5.8	1
152R	199	79	-52	***	-5.0	-3.3	-4.8	-5.8	-30
153R	187	162	-2	***	-7.3	-6.3	-2.4	-3.4	13
154R	185	60	-64	53	-7.5	-7.5	-1.7	-2.4	24
155R	185	46	-44	231	-4.1	-4.4	-3.3	-3.5	-29
156R	150	37	-55	23	-2.7	-3.2	-2.4	-2.7	-51
157R	115	24	-70	6	-3.7	-4.9	10.8	8.3	-27
158R	119	22	-74	5	-1.2	-2.4	12.9	9.1	-70
159R	164	30	-46	8	-3.2	-2.5	-1.4	-1.8	-53
160R	123	32	-41	16	-1.5	-0.9	2.5	1.9	-79
161R	113	31	-45	12	-3.3	-5.2	7.0		-29
162R	123	29	-47	7	3.1	3.7	-0.6	0.0	
166F	250	77	-53	234	-8.4	-5.5	-7.0	-7.2	15
167F	246	113	-32	***	-5.7	-4.6	-5.0	-5.2	-14
168F	164	48	-14	638	-2.2	-3.4	1.9	2.5	-53
169F	168	35	-37	807	-1.7	-2.2	-2.0	-1.2	-67
172R	182	69	-48	72	-7.2	-4.7	-6.4	-8.3	-19
175R	186	59	-56	256	-9.0	-6.7	-5.0	-6.7	6
179R	149	41	-40	20	-4.2	-4.5	-2.8	-0.9	-41
180R	128	16	-63	13	-0.8	-0.2	-0.2	-0.8	103
182R	128	20	-56	18	-1.8	-1.8	-0.4	0.4	-76
183R	95	18	-59	6	-0.5	-0.5	10.0	8.6	-99

APPENDIX C

TABLE OF THEORETICAL FAILURE LOADS

NOTES:

The terms used in this appendix have the following meanings :

Pf	Theoretical failure load.
%EXP	Experimental failure load as a percentage of theoretical.
Pdo	Theoretical failure load with no dent but with measured residual deflection.
%do	Pdo as a percentage of Pf.
Pn	Theoretical failure load with no dent and nominal residual deflection of 1/1000 of span.
%n	Pn as a percentage of Pf.
R	Round impactor.
F	Flat impactor.
S	Failure by axial yield.
M	Failure by mechanism.
U	Failure by structure stiffness matrix becoming unstable.

TEST	Pf	%EXP	Pdo	%do	Pn	%n
44R	458M	15	573M	25	589M	28
45R	464S	10	583S	25	589S	26
46R	465S	20	581S	24	589S	26
47R	454M	21	576M	26	588M	29
48R	445M	25	575M	29	588M	32
49R	449M	24	577M	28	588M	30
50R	442M	25	571M	29	588M	32
51R	444M	33	574M	29	588M	32
52R	436M	24	570M	30	588M	34
53R	410M	10	529M	28	582M	41
54R	429M	5	560M	30	582M	35
55R	424M	12	549M	29	582M	37
56R	383M	16	544U	42	575U	50
58R	368M	14	528U	43	575U	56
59R	346U	21	503U	45	570U	64
61R	319U	23	469U	47	570U	78
62R	384U	18	507S	32	569S	48
63R	389U	27	515S	32	569S	46
64R	377U	26	503S	33	569S	50
65R	361U	0	473U	30	540U	49
70R	321U	23	409U	27	507U	57
78F	518M	21	575M	10	589M	13
79F	520M	15	586M	12	589M	13
80F	515M	19	580M	12	589M	14
82F	482U	-6	500S	3	571S	18
87R	336M	7	434M	29	453M	34
88R	340S	13	443S	30	453M	33
89R	341S	14	444S	30	453M	32
90R	335M	5	442M	32	453M	35
91R	328M	5	440M	34	453M	38
93R	325M	13	440M	35	452M	39
94R	329M	11	448M	36	452M	37
95R	317M	11	432M	36	452M	42
96R	316M	-5	431M	36	448M	41
97R	308M	7	416M	34	448M	45
98R	306M	-4	414M	34	448M	45
99R	274M	9	399U	45	443M	61
100R	268M	7	390U	46	443M	66
101R	277M	1	408U	47	443M	59
102R	224M	21	366U	63	439U	96
103R	228M	11	362U	58	439U	91
104R	223M	12	348U	56	439U	96
105R	263M	-1	377M	40	438M	63
106R	261M	-3	367M	40	438M	67
107R	261M	3	363M	39	438M	68
108R	233U	-10	347U	49	422U	81
110R	209U	-9	319U	52	422U	101
111R	223U	-10	323U	44	411U	84
113R	191U	10	284U	48	411U	115

TEST	Pf	%EXP	Pdo	%do	Pn	%n
121F	380M	19	447M	17	453M	19
122F	380M	16	452M	18	453M	19
123F	379M	12	449M	18	453M	19
124F	303M	5	333M	9	440M	45
125F	313M	-1	353M	11	440M	38
126F	281U	-29	319U	13	421U	49
127F	271U	-20	304U	12	421U	55
130R	249S	17	337S	35	346S	38
131R	244S	9	342S	39	346S	41
132R	242M	-4	337M	39	346M	43
133R	234M	0	331M	41	346M	47
135R	222M	-5	310M	39	342M	54
136R	173M	-15	272U	57	337U	94
137R	164M	-14	258U	56	337U	104
138R	195M	-9	299M	52	336U	71
139R	180M	-3	269M	49	336U	86
140R	124M	1	239U	91	323U	159
145F	277S	22	342S	23	347S	25
146F	273S	7	347S	27	346S	26
147F	258M	-1	299M	15	337M	30
148F	250M	-4	294M	17	337M	34
152R	216S	-8	330S	52	332S	53
153R	221M	-15	321M	45	332M	50
154R	215M	-14	313M	45	332M	53
155R	199M	-7	284M	42	328M	64
156R	194M	-23	292M	50	328M	68
157R	157M	-27	254U	62	324U	106
158R	151M	-21	234U	54	324U	113
159R	170M	-4	261M	53	321M	88
160R	148M	-17	232M	56	321M	116
161R	125U	-10	221U	76	309U	146
162R	111M	11	193U	73	309U	178
166F	250S	0	335S	33	332S	33
167F	232M	6	295M	27	332M	43
168F	207M	-21	255M	23	323M	55
169F	192M	-13	251M	30	323M	67
172R	176S	3	265S	50	263S	49
175R	173S	8	256M	48	262M	51
179R	138M	8	217M	57	258U	86
182R	95M	35	164U	73	248U	160
183R	81M	16	143U	75	248U	203

MAIL ORDER
HSE priced and free publications are available from:
HSE Books
PO Box 1999
Sudbury
Suffolk CO10 6FS
Tel: 01787 881165
Fax: 01787 313995

RETAIL
HSE priced publications are available from good booksellers.

HEALTH AND SAFETY ENQUIRIES
HSE InfoLine
Tel: 0541 545500
or write to:
HSE Information Centre
Broad Lane
Sheffield S3 7HQ

3 0011 Fax 071 873 8200 (counter service only)
3 3740 Fax 021 643 6510
3Q 0272 264306 Fax 0272 294515
834 7201 Fax 061 833 0634
1 Fax 0232 235401
3 4181 Fax 031 229 2734

ISBN 0-11-882130-X

£20.00 net